

Transformation of head structures during the metamorphosis of *Chrysomela populi* (Coleoptera: Chrysomelidae)

SI-QIN GE^{*,1}, YI HUA^{1,2}, JING REN^{1,2}, ADAM ŚLIPÍŃSKI³, BRUCE HEMING⁴,
ROLF GEORG BEUTEL⁵, XING-KE YANG^{*,1} & BENJAMIN WIPFLER¹

¹ Key Laboratory of Zoological Systematics and Evolution, Institute of Zoology, Chinese Academy of Sciences, Beijing, China; Si-Qin Ge [gesq@ioz.ac.cn]; Xing-Ke Yang [yangxk@ioz.ac.cn] — ² University of Chinese Academy of Sciences, Beijing, China — ³ CSIRO Ecosystem Sciences, Australian National Insect Collection, Canberra, Australia — ⁴ University of Alberta, Department of Biological Sciences, Edmonton, Canada — ⁵ Entomology Group, Institut für Spezielle Zoologie und Evolutionsbiologie mit Phyletischem Museum, Friedrich-Schiller-Universität Jena, Jena, Germany — * Corresponding authors

Accepted 11.iii.2015.

Published online at www.senckenberg.de/arthropod-systematics on 17.iv.2015.

Abstract

External and internal head structures of last instar (3rd) larvae, 4th day pupae and adults of *Chrysomela populi* were examined using a combination of traditional and modern morphological techniques, especially μ -computed tomography and computer-based 3D reconstruction. Morphological differences and similarities between the stages were assessed. In addition to long known transformations such as the appearance of compound eyes and the reorientation of the head capsule, the adult differs from the larva by having elongated antennae and palps, a gula and anterior and dorsal tentorial arms. Additionally, several changes in the muscular system occur. Most of these cephalic transformations are related to different tasks playing a predominant role in the developmental stages: feeding in the larvae, and dispersal and mating in the adults, the latter requiring improved sensory perception. The 4th day pupal head shows a combination of adult and larval characters. Almost all adult cephalic elements are already present but the internal anatomy shows several larval traits, especially in the musculature. The central nervous system is intermediate with enlarged optic lobes but still identifiable individual nerves cords. A short historical review on the application of non-invasive methods to study morphological details of metamorphosis is provided and the advantages and limitations of these approaches are discussed.

Key words

Metamorphosis, pupa, larva, morphology, *Chrysomela populi* Linnaeus, X-ray computed tomography, 3D-computer reconstruction.

1. Introduction

Holometabola (= Endopterygota) are an exceptional group of organisms and their origin was referred to as a “nodal point” in insect evolution (HINTON 1977; but see KRISTENSEN 1999). With approximately 800,000 described species they comprise about 2/3s of the known total diversity of animals (GRIMALDI & ENGEL 2005). Bursts of diversification took place in different megadiverse subgroups and different factors played a role, such as an improved flight apparatus or their co-evolu-

tion with angiosperms (GRIMALDI & ENGEL 2005; BEUTEL et al. 2011). Nevertheless, it is likely that complete metamorphosis with larvae differing profoundly from adults and a pupal stage was a crucial feature in the evolution of this megadiverse lineage (e.g., BEUTEL & POHL 2006). This includes ontogenetic specializations including diet, reduced intraspecific competition between juveniles and adults, and more efficient control of development (e.g., GRIMALDI & ENGEL 2005).



Fig. 1. *Chrysomela populi* Linnaeus, photographs: **A:** larva, lateral view; **B:** pupa (pupal sheath with pharate adult inside), lateral view; **C:** adult, lateral view. Scale bar: 2 mm.

Until now, most studies on the metamorphosis of holometabolous insects have been limited to selected model organisms such as the fruit fly *Drosophila melanogaster* (e.g., ROBERTSON 1936; HARTENSTEIN, 1993; WHITE 1999; see also review in HEMING 2003), the mealworm *Tenebrio molitor* (BREIDBACH 1987; see also BREIDBACH 1988), or blowflies (*Calliphora*; CROSSLEY 1965). Even though the external habitus of pupae of a comparatively large number of beetle species have been described and pupal features have occasionally been used in phylogenetic analyses (e.g., ARCHANGELSKY 1997, 1998), very few detailed studies have been carried out on metamorphosis in the extremely successful Coleoptera. A relatively detailed treatment of the pupa of *Dytiscus marginalis* L. was presented in the remarkable two volumes on this species by KORSCHLITZ (1923, 1924) and some related earlier studies (e.g., BAUER 1910). POLILOV & BEUTEL (2009, 2010) compared changes in the hooded beetle *Sericoderus lateralis* (Coleoptera: Corylophidae) and *Mikado* sp. (Coleoptera: Ptiliidae). While their studies covered the larvae, pupae and adults, their main focus was on the effects of miniaturization and phylogeny. Moreover, they omitted detailed information on the anatomy of the pupa. In other endopterygote groups comparative morphological data are equally scarce. OERTEL (1930) provided a detailed account of the transformations of the skeleton, digestive- and muscular systems in the honeybee *Apis mellifera*, but omitted detailed information on cephalic musculature. It is apparent that the pupal stage, an instar characterized by major reconstruction of most body parts and organs, is crucial to better understanding complete metamorphosis. The morphological transformations occurring during metamorphosis are presently still very insufficiently known.

In recent studies (DEANS et al. 2012; LOWE et al. 2013; FRIEDRICH et al. 2014) it was shown that computed tomography (μ -CT) is a valuable tool to study insect anatomy. Experiments carried out at the Institute of Zoology of the Chinese Academy of Sciences confirm that it also greatly facilitates the study of the pharate adult within the pupal sheath. This and the conspicuous lack of information on metamorphosis in beetles induced us to execute this comparative study of the skeleto-muscular system of the head. It covers crucial stages of the life cycle of

Chrysomela populi (Coleoptera, Chrysomelidae): the final larval instar, the pupal stage (day four), and the adult (Fig. 1A–C).

For this investigation we chose this species for several reasons. First, it belongs to the species rich phytophagan superfamily Chrysomeloidea (ca. 67,000 known spp.). KRISTENSEN (1999) emphasized that Phytophaga, i.e. Chrysomeloidea and Curculionoidea, constitute one of the truly megadiverse holometabolan lineages. Chrysomelid beetles exclusively feed on plant materials, usually on green parts, but members of some subgroups secondarily switched to pollen, flowers, or seeds (JOLIVET & VERMA 2002). FARRELL (1998) hypothesized that angiosperm feeding may have been the principal cause for the success of this group, an evolutionary correlation that probably also applies to glossatan Lepidoptera (KRISTENSEN 1999). Therefore herbivory and the successful co-evolution with angiosperms may have been critical to “megadiversification” in these lineages of Holometabola. Aside from their great economic importance (JOLIVET & VERMA 2002) chrysomelids are widely recognised as a model for plant-herbivore co-evolution (EHRlich & RAVEN 1964; MITTER & FARRELL 1991; BECERRA 1997; XUE et al. 2008, 2009). Another point in favour of examining Chrysomelidae and *Chrysomela populi* is the well-established leaf beetle research group at the Institute of Zoology of the Chinese Academy of Sciences, with taxonomic and morphological expertise, rich preserved material, and with well-established rearing facilities. Finally, *C. populi* was chosen to honour the outstanding 18th century biologist Carolus Linnaeus, who described it as the first chrysomelid species, the type species for the entire family.

Morphological studies on chrysomelid beetles and their immatures are surprisingly scarce. Structural features of larvae and adults were examined by RIVNAY (1928), MAULIK (1926), MANN & CROWSON (1981, 1983, 1984, 1996), COX (1981, 1988, 1996), REID (1995, 2000), SUZUKI (1996), SAMUELSON (1996), SCHMITT (1998), HEIDENREICH et al. (2009), KLASS et al. (2011) and HÜBLER & KLASS (2013). However, the information provided on internal structures such as the musculature remained scarce, and virtually no information was available on the anatomy of pupae and on the changes undergone by

internal structures during metamorphosis. The primary goal of this work is to provide a detailed description of the skeleto-muscular system of the head of the last (3rd) instar larvae, pupae and adults of a well-known species. Other character systems such as nervous system, digestive system, sensilla or glands were only treated incompletely. Additionally, the potential and limitations of non-invasive methods in the study of metamorphosis are evaluated. A broad description of all events occurring during the pupal stage is presently in preparation, but is beyond the scope of this study and will be presented separately.

2. Materials and methods

Examined specimens. Mature larvae and adults of *Chrysomela populi* Linnaeus (Fig. 1) were preserved in 75% ethanol. They were collected in May 2012 in Shuiquangou, Dazhuangke, Yanqing, Beijing, People's Republic of China. Larvae from the same locality and date were reared in glass jars (12 × 11.5 cm) with sand on the bottom and a sufficient supply of host plants. Fresh plant leaves were added every day and wilted leaves removed. The containers were kept closed except for feeding and removing old material, at a constant temperature of 25°C, 16 hours of light and 8 hours of darkness, and a humidity of around 80%. The pupae were collected 4 days after the mature larvae pupated and fixed for morphological study. The adult specimens were killed of day after hatching. All collected specimens were identified by the first author.

X-ray computer tomography. Species used for x-ray micro-computed tomography (μ-CT) were dehydrated with ethanol (75–100%) and acetone and dried at the critical point (Hitachi hcp-2). One fourth day pupa and one adult were scanned with a Skyscan 2010 μ-CT at the Beijing Institute of Technology (beam strength: 40 keV, absorption contrast), while the larva was scanned with an X-radia 200 at Shanghai Jiaotong University (beam strength: 40 keV, absorption contrast).

Three-dimensional reconstruction (3D). Micro-CT images were used for 3-dimensional reconstructions. Based on the obtained image stacks, structures of the larva, pupa and adult were reconstructed with Amira 5.4 for Figs. 4, 7 & 11. The data files were then transferred to Maya 2013 (Autodesk) in order to use the smoothing function, and the specific display, and rendering options implemented in this software. Material separation for figure 6 was done with Amira 5.4 (Visage Imaging) and subsequent rendering was performed with VG Studiomax 2.1 (Volume Graphics). Final figures were prepared with Photoshop and Illustrator (CS5, Adobe).

Photography. Habit photos of the larvae, pupa and adult were taken with a D300s Nikon camera connected to

the stereoscope (Zeiss Stereo Discovery V12). Final figures were prepared with Photoshop and Illustrator (CS5, Adobe).

Scanning electronic microscopy (SEM). Specimens were transferred to 100% ethanol, then dried at the critical point (critical point dryer: Leica EM CPD 300) and subsequently sputter-coated (Leica EM SCD 050). Microscopy was performed on a FEI Quanta 450. Final figures were prepared with Photoshop and Illustrator (CS5, Adobe).

Histological sections. One adult head was embedded in Araldite® (Huntsman Advanced Materials, Bergkamen, Germany) for semi-thin sectioning (1 μm) with a glass knife on a microtom HM 360 (Microm, Walldorf, Germany). The sections were stained with toluidin-blue. Images of sections were taken with a Zeiss Axioplan (Zeiss, Göttingen, Germany).

Terminology. We used the general terminology of BEUTEL et al. (2014). The muscles are subsequently numbered with a prefixed letter indicating the developmental stage: an “l” in the larva, a “p” in the pupa and an “a” in the adult. In the discussion (Table 4), muscles are named according to the terminology of WIPFLER et al. (2011).

3. Results

In the following sections external features and internal organ systems including the central nervous system, the musculature and the cephalic digestive tract are described for final instar larvae, 4th day pupae and adults of *Chrysomela populi*.

3.1. Mature larva

Figs. 1–4

General body shape similar to that of pupa and adult (Fig. 1A). Moderately elongate, not compressed dorso-ventrally; abdomen evenly narrowing towards apex, lacking urogomphi. Head, legs and pronotum strongly sclerotized and very darkly pigmented; remaining body surface with a conspicuous pattern of membranous pink integument armored with numerous sclerotized and darkly pigmented setiferous plates.

Head capsule. (Figs. 2, 4) Orthognathous, angle between longitudinal body axis and longitudinal axis of head (between top of head and mandibular apex) 88°. Head capsule heavily sclerotized. Coloration black except for few less sclerotized parts. Six stemmata (ste; Figs. 2A,E, 4A,C) present on each side of head, four (ste1–4; Fig.

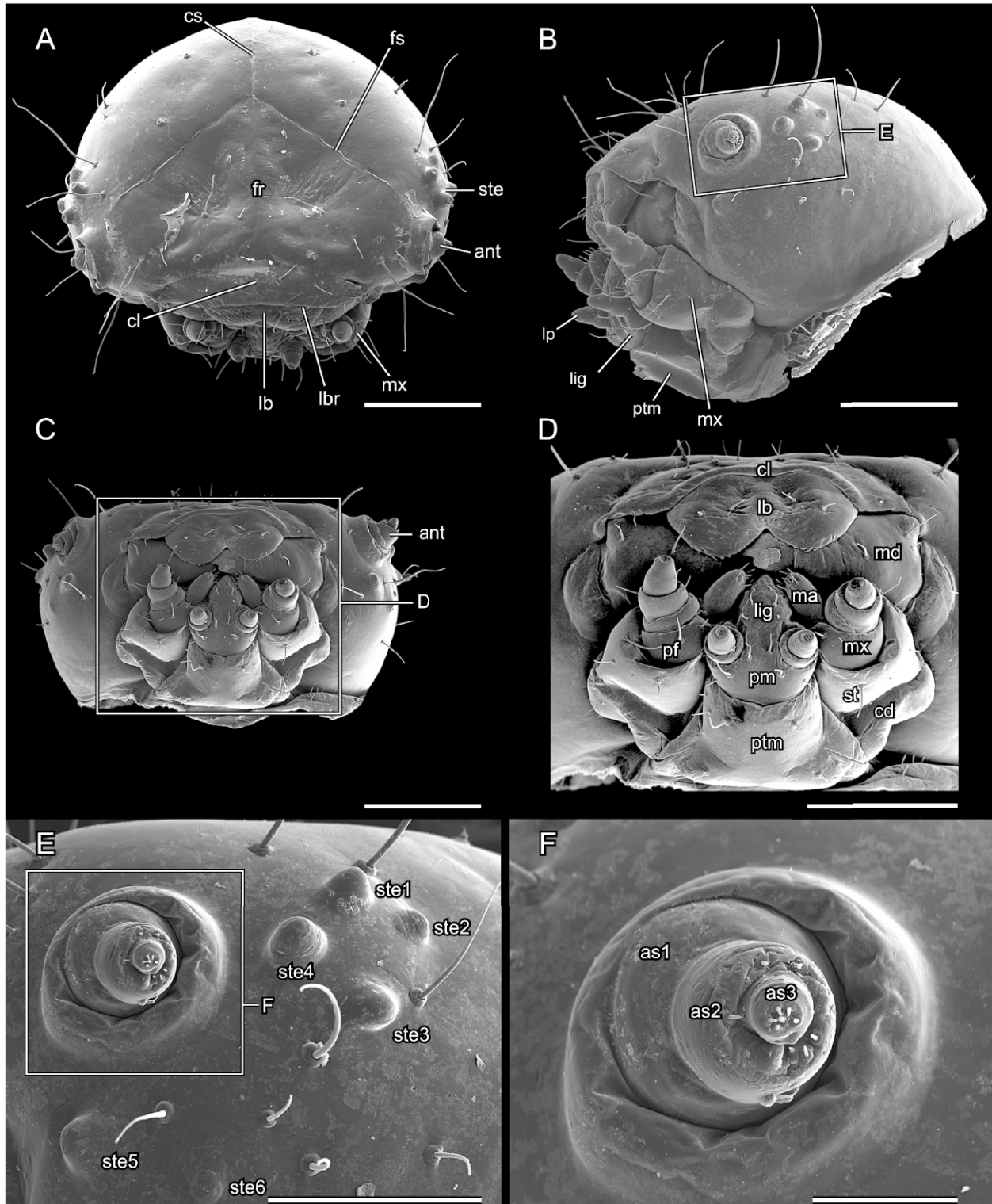


Fig. 2. Mature larva (3rd instar) of *Chrysomela populi*, SEM micrographs. **A:** head, dorsal view; **B:** head, lateral view; **C:** head, frontal view; **D:** mouthparts, frontal view; **E:** antenna and stemmata, lateral view; **F:** apex of antenna. — **Abbreviations:** ant: antenna; as1, as2, as3: antennal segment 1, 2, 3; cd: cardo; cl: clypeus; cs: coronal suture; fr: frons; fs: frontal suture; lb: labrum; lbr: clypeo-labral ridge; lig: ligula; lp: labial palp; ma: mala; md: mandible; mx: maxilla; pm: prementum; ptm: postmentum; st: stipes; ste: stemmata; ste1, 2, 3, 4, 5, 6: stemmata 1, 2, 3, 4, 5, 6. Scale bar: A–D: 1 mm, E: 0.3 mm, F: 0.1 mm.

2E) forming a group behind the antenna and two below the antennal base (ste5–6; Fig. 2E). Epicranial suture distinct, Y-shaped; coronal suture (cs; Fig. 2A) about 1/3

as long as length of dorsal head capsule; frontal sutures (fs; Fig. 2A) forming a wide angle with each other, with very slight irregularities, reaching antennal sockets an-

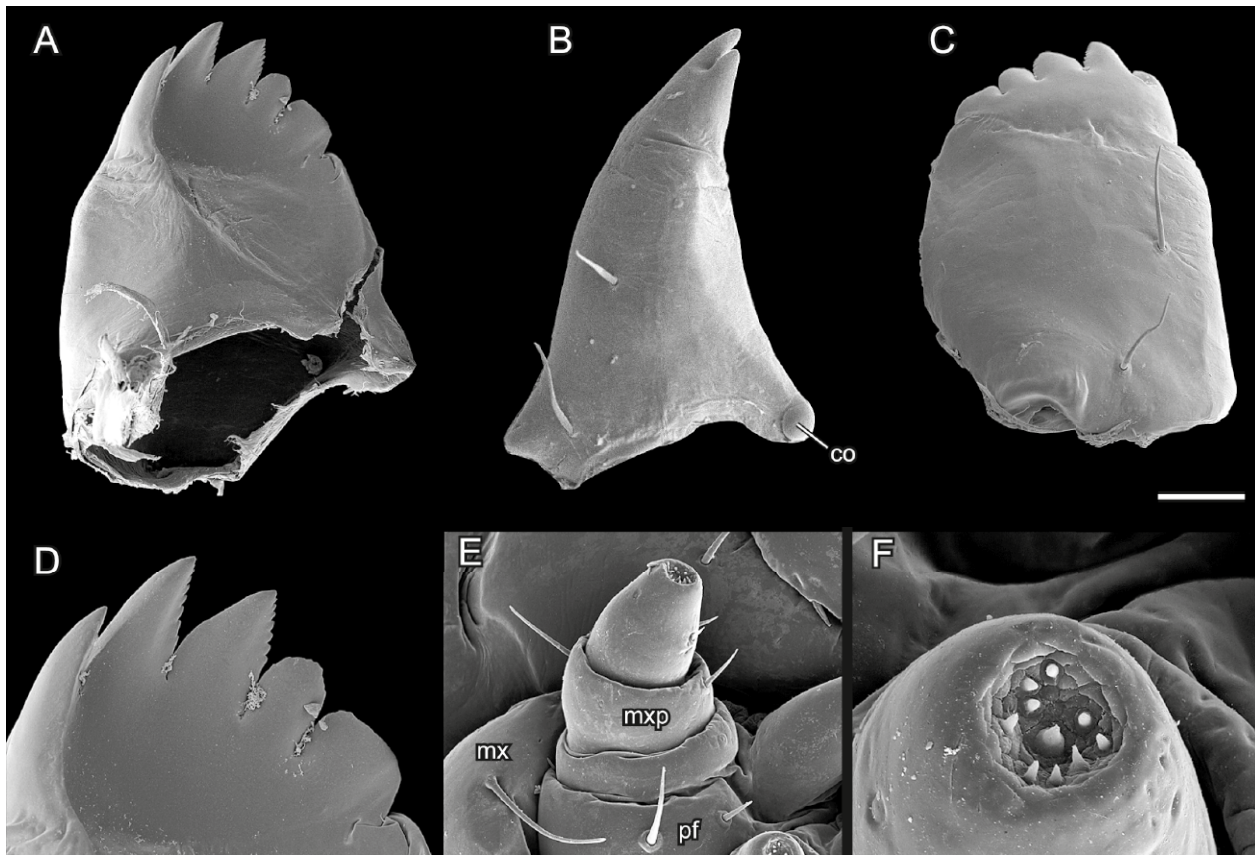


Fig. 3. Mature larva (3rd instar) of *Chrysomela populi*, SEM micrographs. **A:** mandible, ventral view; **B:** mandible, lateral view; **C:** mandible, dorsal view; **D:** distal part of mandible, ventral view; **E:** maxillary palp; **F:** distal part of maxillary palp. — **Abbreviations:** co: condyle; mx: maxilla; mxp: maxillary palp; pf: palpifer. Scale bar: A–D: 1 mm, E: 0.1 mm, F: 0.03 mm.

terolaterally; median endocarina extending from base of frontal sutures to clypeus. Frons broad (fr; Fig. 2A). Frontoclypeal strengthening ridge distinctly recognizable externally, slightly concave. Clypeus (cl; Figs. 2A, 4G) roughly trapezoid, nearly four times as wide as long, with rounded lateral edges. Foramen occipitale wide, enclosed by well-developed postoccipital ridge dorsally and laterally (por; Fig. 4G). Hypostomal rods and ventral epicranial ridges absent. Gula or hypostomal bridge absent, posterior labial margin contiguous with ventral cervical membrane. Internal surface of frons with Y-shaped sclerotized structure with short basal part.

Cephalic endoskeleton. Tentorium represented only by posterior arms, which are connected internally by a corpotentorium (pta; Fig. 4G); Anterior and dorsal arms missing.

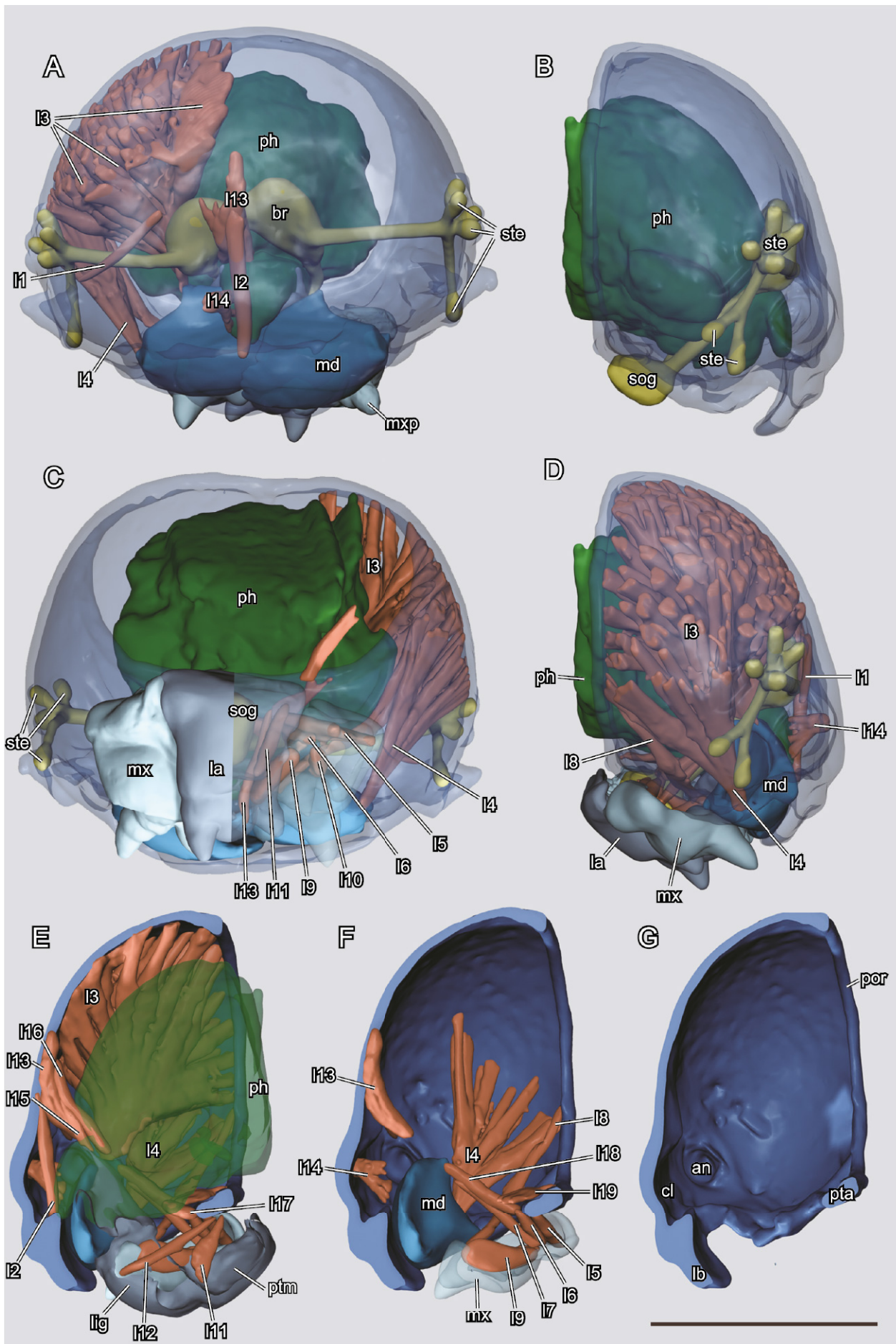
Labrum and epipharynx. Labrum (lb; Figs. 2A,D, 4G) movably connected with anterior clypeal margin by internal membranous fold; orientation almost vertical. Transverse, sclerotized, with rounded lateral edges and deep antero-median notch. Labral lumen subtrapezoid in cross section. Anterior epipharynx slightly convex, with shallow median edge and strongly developed but relatively short paramedian sclerotized tormae.

Antennae. Antenna (ant; Fig. 2A,C) short and 3-segmented (as1–3; Fig. 2F). Insertion areas located at

lateral ends of frontal sutures; bulged, round articular membrane broader posteriorly than anteriorly (Fig. 2E,F). Proximal antennomere short, ring-shaped; second antennomere twice as long as first, with conical sensory papilla and six sensilla of different size; distal antennomere elongate, narrow, with six long sensilla on its apical surface.

Mandibles. Mandibles symmetrical and palmate (md; Figs. 2D, 3A–D, 4A,D,F), strongly sclerotized, with typical dicondylic articulation (i.e., with dorsal acetabulum/socket and ventral condyle). Distally with five teeth arranged in a nearly vertical row, three of them more prominent, apically pointed and serrated along their lateral edges; two proximal teeth less prominent and blunt; indistinct serration only recognizable on distal one. Penicillus, prosthema and mola absent.

Maxillae. Maxilla retracted, inserted in deep maxillary articulating area between postmentum and ventrolateral wall of head capsule. Narrow triangular section of articular membrane visible externally, laterad of submentum and posterior to mentum. Cardo large, broadly triangular. Stipes almost two times as long as cardo, slightly narrower, undivided; with long seta on ventral side and additional seta on broad lateral surface. Mala distinct, sclerotized, shaped like a large, apical palpomere. Palpifer present, large, appearing palpomere-like in ventral



← **Fig. 4.** Mature larva (3rd instar) of *Chrysomela populi*, 3D reconstructions of internal structures. **A:** frontal view, cuticle rendered transparent; **B:** lateral view, cuticle rendered transparent, muscles removed; **C:** posterior view, cuticle rendered transparent, right half of labium and right maxilla rendered transparent; **D:** lateral view, cuticle made transparent; **E:** mid-sagittal section, pharynx; **F:** mid-sagittal section, pharynx, labium and parts of musculature removed, maxilla rendered transparent; **G:** mid-sagittal section, head capsule only. — **Abbreviations:** br: brain; cl: clypeus; I1–I19: musculature; lb: labrum; lig: ligula; lp: labial palp; md: mandible; mx: maxilla; mxp: maxillary palp; ph: pharynx; por: postoccipital ridge; pta: posterior tentorial arms; sm: submentum; sog: suboesophageal ganglion; ste: stemmata. Scale bar: 1 mm.

Table 1. Musculature of the larva of *Chrysomela populi*.

Number	Origin	Insertion	Function
I1	dorsal wall of head capsule	postero-dorsal margin of scape	levator of the antenna
I2	frons	medially on ventral labral wall	depressor of the labrum
I3	broadly on dorsal and lateral wall of head capsule	with a tendon on median mandibular wall	adductor of the mandible
I4	lateral wall of head capsule	with a tendon on lateral mandibular wall	abductor of the mandible
I5	tentorium	with several bundles along entire wall of cardo	promotor of the maxilla
I6	anterior side of tentorial bridge, directly anterad I5	stipes, very close to stipitocardinal ridge	promotor of the maxilla
I7	oral arm of hypopharynx	stipes, anterad I6	promotor of the maxilla?
I8	lateral wall of head capsule, directly ventrad of Omd1	basal edge of mala	adductor of the mala
I9	stipital wall	basal edge of mala	adductor of the mala
I10	lateral stipital wall, close to I9	ventro-lateral edge of palpomere 1	flexor of the maxillary palp
I11	anterio-ventral area of tentorial bar	latero-basal edge of prementum	retractor of the prementum
I12	anterior side of tentorium, slightly dorsad of I11	area in between labium and ligula	retractor of the prementum
I13	frons, directly posterad I2	oral arms of hypopharynx	elevator of the hypopharynx
I14	ventral frons, slightly dorsad clypeofrontal ridge	epipharyngeal wall, anterad frontal ganglion	dilator of the cibarium
I15	frons, laterad I12	dorsal side of pharynx	dilator of the pharynx
I16	frons, posterad I15	dorsal side of pharynx, directly anterad brain	dilator of the pharynx
I17	anterior region of tentorial bridge	ventral side of pharynx	dilator of the pharynx
I18	anterior region of tentorial bridge, laterad I17	ventral side of pharynx, posterad I17	dilator of the pharynx
I19	area between posterior tentorial arms and head capsule	ventral pharyngeal wall, close to insertion of I17	dilator of the pharynx
I20		ring muscle layer around pharynx	constrictor of the pharynx
I21		longitudinal muscle layer along pharynx	contractor of the pharynx

view but not closed mesally; longer seta inserted ventrally and short seta close to mesal edge. Maxillary palp (mxp; Figs. 3E, 4A) 3-segmented; basal palpomere short, ring-shaped; palpomere 2 slightly narrower but longer than basal one; apical palpomere about as long as proximal ones, conical; apical concavity with 11 sensilla (Fig. 3F); all palpomeres without digitiform sensilla.

Labium. Anterior labium and hypopharynx fused, forming a labiohypopharyngeal complex or prelabium. Postmentum (ptm; Figs. 2B,D, 4E) broad and trapezoid, largely undivided; border between submentum and mentum only recognizable close to lateral margin. Broad posterior postmental margin adjacent to cervical membrane (see above). Anterior region of postmentum subparallel, connected with posterior premental margin by internal membrane. Prementum well developed, subparallel. Palpiger absent. Palp 2-segmented, slightly smaller than two distal maxillary palpomeres combined; proximal palpomere short but wider than apical one; apical palpomere conical, similar to apical maxillary palpomere, with apical concavity with 10 sensilla. Ligula (lig) prominent, continuous with premental wall, enclosed by malae and reaching their apices; weakly sclerotized; apex pointed and almost reaching mandibular teeth. Paired tube-like

glands (usually present in cucujiform larvae) not recognizable in μ -CT images, apparently absent.

Pharynx. Posterior prelabiohypopharyngeal complex and posterior epipharynx not fused, closed prepharyngeal tube absent. Pharynx (ph; Fig. 4B,C–E) very wide, diameter at least 52% of diameter of head capsule, filling out a large parts of central and posterior lumen of head; shape almost quadrangular in cross section, without distinct longitudinal folds for attachment of dilators.

Cerebrum and suboesophageal ganglion. Brain (br; Fig. 4A) located in anterior head region, small in relation to entire cephalic lumen. Two hemispheres rather compact. Recognizable external boundaries between proto-, deuto- and tritocerebrum including tritocerebral commissure not visible. Moderately thick optic tracts arise from lateral protocerebral region; shortly before reaching lateral wall of head capsule dividing into six separate optic nerves, arranged according to position of stemmata (Fig. 4A–C). Suboesophageal ganglion (sog; Fig. 4B,C) small in relation to head size; larger part located in postero-ventral part of head capsule, partly shifted to prothorax.

Musculature. The musculature of the larva is illustrated in Fig. 4 and described in Table 1.

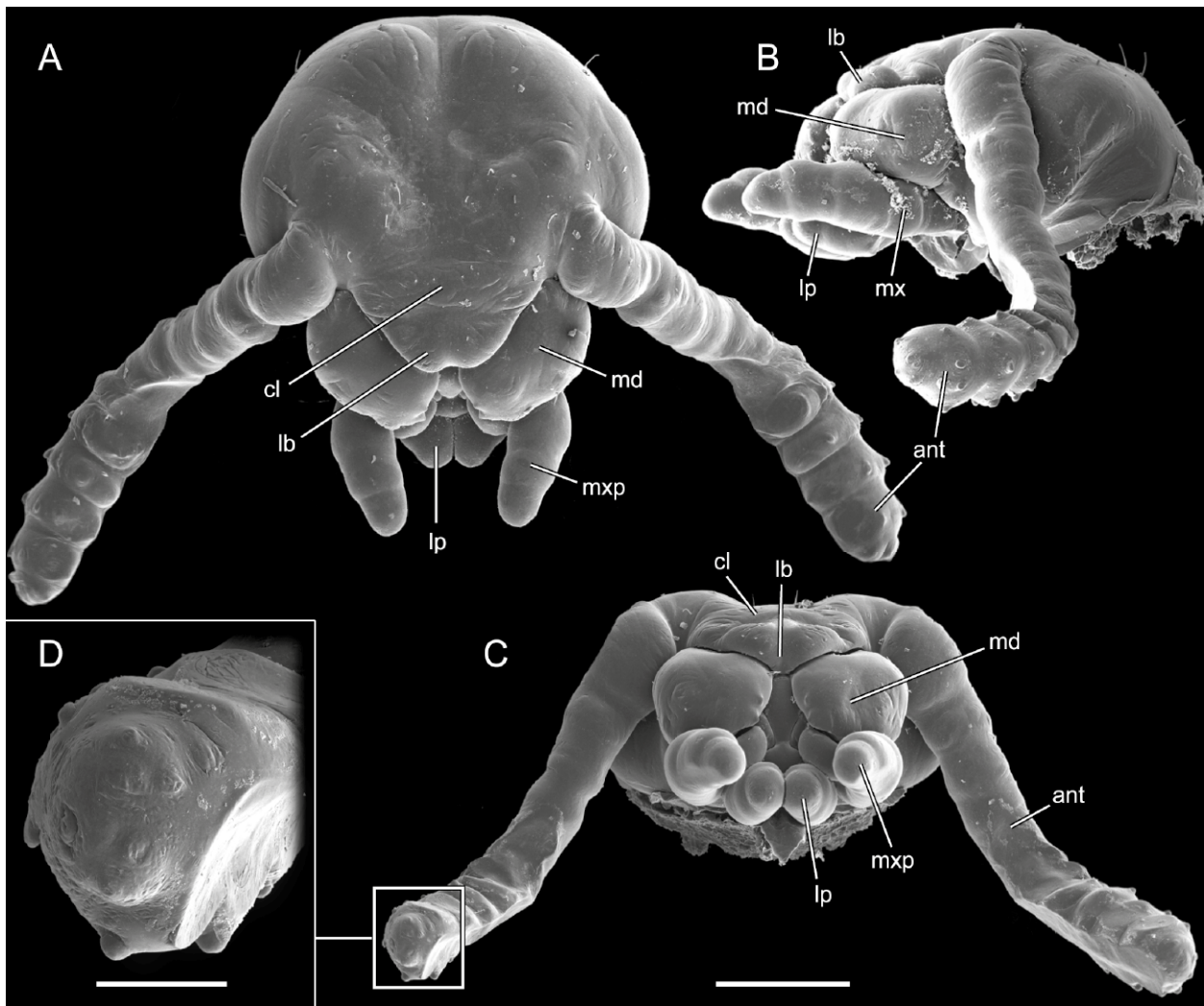


Fig. 5. Pupa of *Chrysomela populi*, SEM micrographs. **A:** head, dorsal view; **B:** head, lateral view; **C:** head, frontal view; **D:** distal part of antenna. — **Abbreviations:** ant: antenna; cl: clypeus; lb: labrum; lp: labial palps; md: mandible; mx: maxilla; mxp: maxilla palps. Scale bars: A–C: 0.5 mm, D: 0.1 mm.

3.2. 4th day pupa

Figs. 5–7

Pupa immobile and of adecticous exarate type, lacking urogomphi (Fig. 1B). Body oval, convex dorsally. Coloration pale yellow with many large black dots (Fig. 1B). Pharate adult well developed within pupal sheath (4th day pupa) (consequently all internal structures are treated below under 3.2.2. Pharate adult within pupa).

3.2.1. Pupal sheath

Head capsule. Head (Figs. 5A,B, 6A–C) strongly inflected, hypognathous, not visible from above. Coloration mostly black, but posterior cephalic parts yellowish brown. Evenly rounded laterally and posterolaterally, distinctly narrowing towards foramen occipitale. Compound eyes recognizable as indistinct kidney-shaped swelling posterior to basal antennomeres. Shallow con-

vexities above antennal bases separated by flat median frontal region; paired moderately convex halves of vertex separated by indistinct coronal suture. Sheath smooth and largely glabrous. Frontal suture not recognizable. Clypeofrontal ridge very indistinctly recognizable externally. Clypeus transverse. Articulation of labrum and antenna (ant; Fig. 5A–D) indistinct. Mouthparts distinctly developed and exposed, but individual elements such as endite lobes or palpomeres not clearly defined.

Labrum. Labrum (lb; Fig. 5A–C) with strongly converging lateral margins, smoothly rounded anterolateral edges, and median emargination; length ca. 0.4 × basal width; clypeolabral suture indistinct laterally, not recognizable medially.

Antennae. Antenna widening towards apex. Subdivision into antennomeres scarcely recognizable proximally, slightly more distinct between antennomeres 8–11. Distal five antennomeres with distinct tubercles; mesal and dorsal surface flattened; apex of terminal antennomere with papillae (Fig. 5C,D).

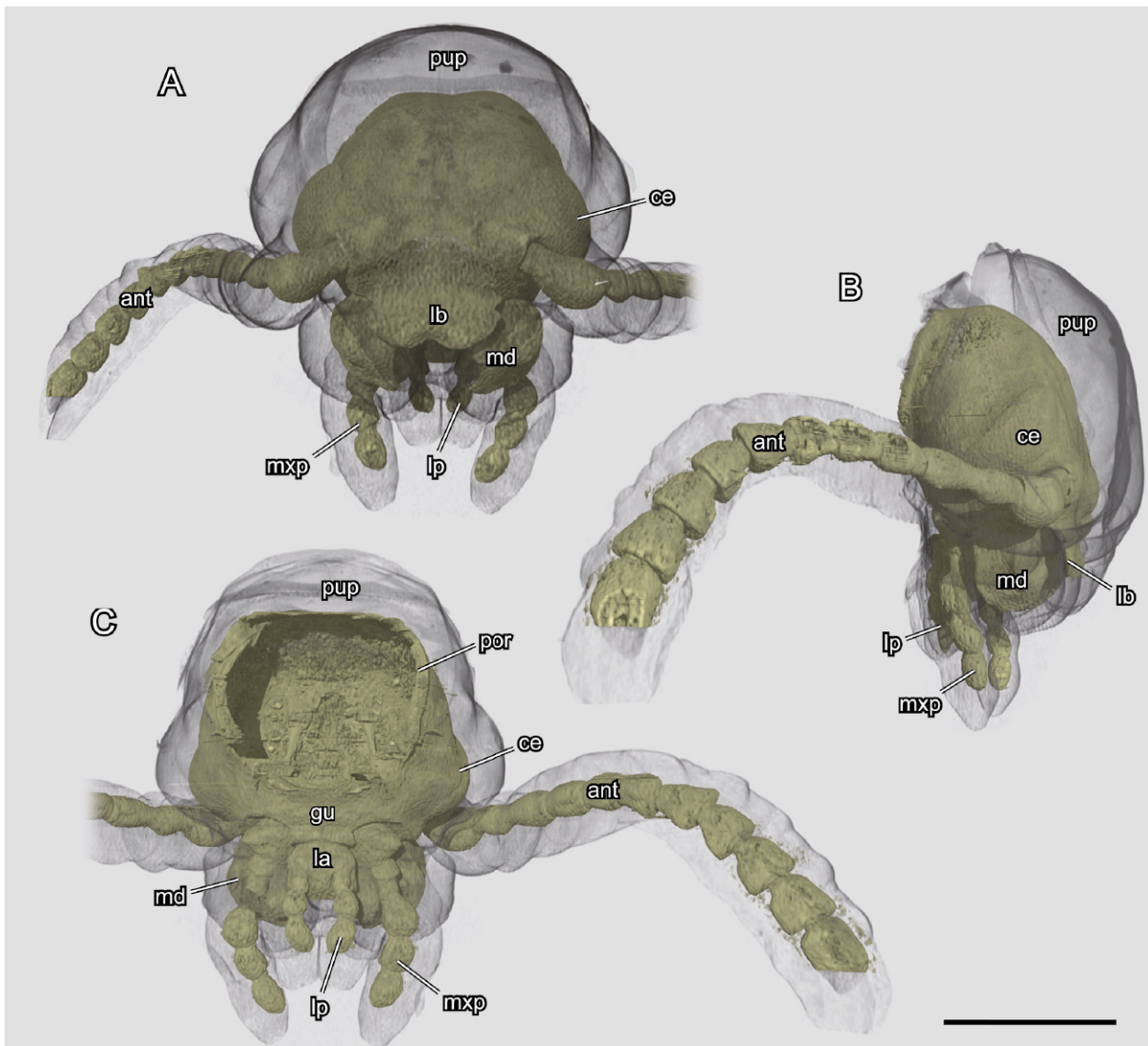


Fig. 6. Pupa and pharate adult of *Chrysomela populi*, 3D reconstructions, pupal sheath rendered transparent. **A:** anterior view; **B:** lateral view; **C:** posterior view. — **Abbreviations:** ant: antenna; ce: compound eye; gu: gula; la: labium; lb: labrum; lp: labial palp; md: mandible; mx: maxilla; mxp: maxillary palp; por: postoccipital ridge; pup: pupal sheath. Scale bar: 1 mm.

Mandibles. Mandibles well developed and largely exposed. Visible part (md; Fig. 5A–C) almost globular, with two small pointed tubercles apically.

Maxillae. Individual elements not distinctly separated and closely adjacent with labium mesally. Segmentation of maxillary palp (mxp; Fig. 5A,C) only vaguely indicated; setae, tubercles or papillae absent. Endite lobes undifferentiated, together placed between lower surface of mandibles, maxillary and labial palps.

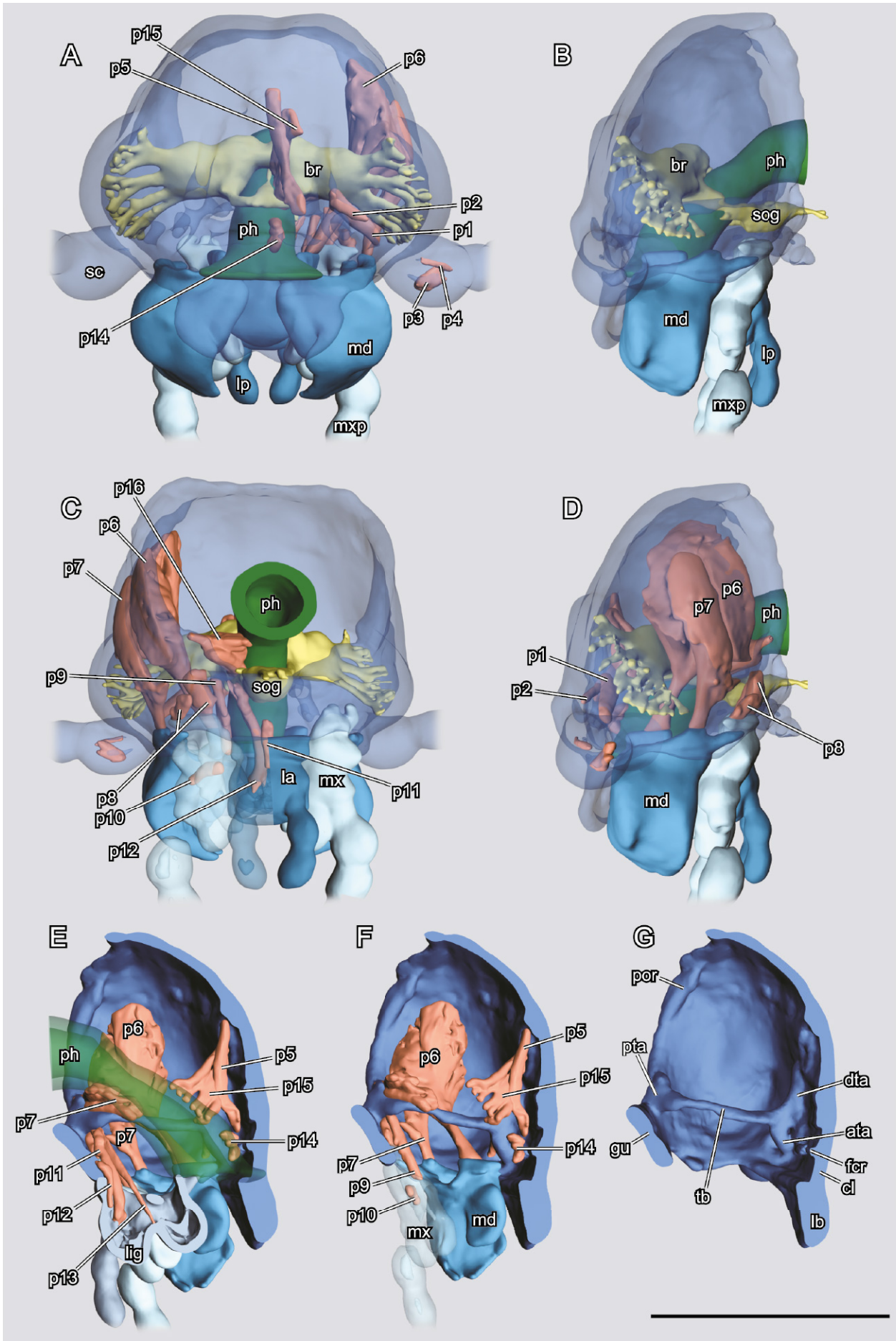
Labium. Labial elements not distinctly separated. Palps (lp; Fig. 5A–C) similar to those of maxillae but shorter.

3.2.2. Pharate adult within pupal sheath

Head capsule. In between orthognathous and subprognathous, angle between longitudinal body axis (indicated by foramen occipitale) and mouthparts 128° , separated

from pupal sheath by fairly wide space filled with liquid, distinctly smaller than pupal sheath. Head much more rounded than in adult laterally and posteriorly. Cephalic sutures indistinct. Compound eyes kidney-shaped and distinctly visible. Antennal insertion more dorsad. Suture separating posterior submentum from ventrolateral wall of head capsule not visible. Gula present, transversely extended, short and broad, anteriorly fused with submentum (gu; Fig. 6C); internal gular ridge and posterior tentorial groove not distinguishable. Foramen occipitale large dorsally but distinctly less wide than maximum width of head capsule; dorsally and laterally enclosed by well-developed postoccipital ridge.

Cephalic endoskeleton. Long and slender tentorial bars (tb; Fig. 7G) arising on each side from lateral sides of gula. Anterior arms (ata; Fig. 7G) short and massive, attached to head capsule nearly along their entire length.



← **Fig. 7.** Four day pharate adult of *Chrysomela populi*, 3D reconstructions of internal structures. **A:** frontal view, cuticle rendered transparent; **B:** lateral view, cuticle rendered transparent, muscles removed; **C:** posterior view, cuticle rendered transparent, right half of labium and right maxilla rendered transparent; **D:** lateral view, cuticle rendered transparent; **E:** midsagittal section, pharynx made transparent; **F:** midsagittal section, pharynx, labium and parts of musculature removed, maxilla rendered transparent; **G:** midsagittal section, head capsule only. — **Abbreviations:** ata: anterior tentorial arm; br: brain; cl: clypeus; dta: dorsal tentorial arms; fcr: frontoclypeal; gu: gula; lb: labrum; md: mandible; mxp: maxillary palp; ph: p1–p16: musculature; pharynx; por: postoccipital ridge; pta: posterior tentorial arm; sc: scapus; sog: suboesophageal ganglion; tb: tentorial bar. Scale bar: 1 mm.

Table 2. Musculature of the 4 day pharate adult of *Chrysomela populi*.

Number	Origin	Insertion
p1	anterior and dorsal tentorial arm	ventral base of antenna
p2	dorsal tentorial arm	dorsal base of antenna
p3	dorsal scapal wall	lateral edge of pedicel
p4	dorsal scapal wall	mesal edge of pedicel
p5	mesally on posterior frons	antero-lateral frons, in between anterior and dorsal tentorial arms
p6	lateral and dorsal head capsule	with a tendon on median mandibular wall
p7	lateral head capsule, ventrad p6	with a tendon on lateral mandibular wall
p8	in 2 distinct bundles on latero-ventral head capsule, partly on tentorial bar	cardinal process, bundle 1 on edge of the process, bundle 2 on its distal margin
p9	ventro-lateral head capsule, close origin of tentorial bar	basal edge of lacinia
p10	mesal stipital wall	mesally on palpomere 1
p11	base of tentorial bar	basal edge of prementum
p12	gula	latero-basal edge of prementum
p13	base of tentorial bar, close to p11	dorsal labial area, border to ligula
p14	frons	inner epipharyngeal wall
p15	mesally along frons	along dorsal pharynx, anterad brain
p16	base of tentorial bar	ventral side of pharynx

Dorsal arms (dta; Fig. 7G) longer than anterior ones and also massive. Also attached to head capsule along almost their entire length. Corpotentorium and posterior arms absent.

Labrum and epipharynx. Labrum (lb; Figs. 6A–B, 7G) sclerotized, short, approximately trapezoid, with strongly rounded anterolateral edges and median emargination. Epipharynx membranous, with well-developed median longitudinal bulge.

Antennae. Inserted below oblique anterolateral edge of head capsule (ant; Fig. 6A–C), anterior to compound eyes; antennifer not present. Moderately long, posteriorly almost reaching bases of elytra, composed of scapus, pedicellus, and nine distinct flagellomeres. Scapus (sc; Fig. 7A) longer than all other antennomeres except apical one; articulatory part separated from larger club-shaped distal portion by indistinct impression; anterior edge strongly rounded, posterior edge almost straight; surface of distal part smooth. Pedicellus smaller than scapus, shorter than following antennomeres; with narrower basal part and broader, larger distal portion. Flagellomere 1 similar to pedicellus but longer apically, distinct ring-shaped basal bulge invisible; flagellomere 2 similar but slightly shorter; flagellomere 3 similar in shape to 2; flagellomere 4 shaped like elongate cup; with smooth basal part and widened distal portion; flagellomeres 5–8 similar, but increasing in size and basal portion shorter; apical antennomere as large as scapus; with short basal

part; middle region cylinder-shaped and distal part conical. Pubescence of antennae invisible.

Mandibles. Slightly asymmetric mandibles (md; Figs. 6A–C, 7A,B,D,F) strongly sclerotized, stout, roughly triangular in dorsal view, with rounded lateral margins. External side broad at base and narrowing anteriorly. Distal part of mandible divided into three well-developed, roughly triangular teeth arranged in a vertical row (Fig. 7B,F); middle tooth larger than others, with oblique, slightly irregular edge; dorsal tooth about equally long, more acuminate; ventral tooth quite distant from mandibular apex and blunt.

Maxillae. Maxilla (mx; Fig. 7C,F) composed of cardo, stipes, galea and lacinia and palp. Borders between subelements indistinct. Cardo small, subtriangular, with oblique anterior edge. Stipes with triangular lateral bulge, subdivided into basi- and mediostipes by basally obliterated not recognizable suture. Lacinia and galea present. Proximal galeomere parallelogram-shaped in ventral view; distal galeomere inserted in distal articulation area of galeomere 1; apically rounded. Palpifer weakly developed, laterally adjacent to stipes and proximal galeomere; comparatively small but distinctly visible in ventral view and well-sclerotized. Palp (mxp; Figs. 6A–C, 7A,B) composed of four relatively thick segments, longer than distance from cardinal base to distal margin of galea; palpomere 1 short, inserted on palpifer; palpomere 2 about twice as long, distally widening, with strongly

convex posterior margin, thus appearing curved inwards; palpomere 3 similarly shaped but slightly shorter; palpomere 4 about as long as 2, spindle-shaped; widening after shallow constriction in proximal third; evenly narrowing towards apex; apical region rounded, with anteriorly oriented.

Labium. Labium composed of submentum, mentum and prementum. Submentum large, fused with adjacent regions of head capsule laterally; posterior part moderately converging anteriorly, laterally delimited by rather indistinct furrow; anterior part adjacent to maxillary articulating area, lacking defined lateral border. Mentum small, transverse; connected with anterior submental margin; anterior and posterior margins almost straight. Prementum well-developed, about as large as mentum; cranial edge round (ligula). Palpiger not clearly distinguishable. Labial palp (lp; Fig. 6A–C, 7A,B) similar to maxillary palp, but 3-segmented and shorter; palpomere 1 short and stout, cylindrical; palpomere 2 similar to maxillary palpomere 2 but slightly smaller; apical palpomere 3 very similar to terminal maxillary palpomere.

Pharynx. Pharynx of pharate adult round to oval in cross section, its diameter at least 19% of head capsule.

Cerebrum and suboesophageal ganglion. Brain of pharate adult in central head region, occupying only a small part of entire cephalic lumen. Pars intercerebralis of brain narrow. Protocerebral hemispheres continuous with compact proximal parts of developing optic lobes; lobes laterally branching repeatedly before reaching developing compound eye, thus forming a bush-like pattern (Fig. 7A–B). Recognizable external boundaries between proto- and deutocerebrum not distinguishable. Tritocerebral commissure present. Circumoesophageal connectives broader than in adult. Suboesophageal ganglion small, located in posteroventral head region.

Musculature. The musculature of the pupa (within the pharate adult, see above) is illustrated in Figure 7 and described in Table 2. In some cases muscle bundles and fibers not well developed and generally muscles appear frayed. Additionally some muscles do not attach to the cuticle.

3.3. Adult

Figs. 8–11

Fully sclerotized, without exposed membranes (Fig. 1C). Intensive coloration, with red elytra and other exposed body parts black. Distinctly convex, especially on dorsal side.

Head capsule. Subprognathous, slightly inclined, angle between longitudinal body axis (indicated by foramen occipitale) and mouthparts 154°, as wide as anterior pronotal emargination. Posterior half retracted into prothorax (Fig. 1C). Shape almost square, about as wide as long, with parallel lateral margins behind compound eyes; posterior edges rounded; anterior part in front of compound eyes, short and broad, trapezoid (Fig. 8A). Strongly scler-

otized, with thick cuticle. Setation as shown in Figure 8; longer setae absent except for clypeus; anterior half with fairly dense pattern of punctures; these less dense and less distinct on smooth surface of retracted posterior half of head capsule (Fig. 8A). Circumocular ridge scarcely recognizable externally but well developed internally; supraorbital suture absent. Compound eyes (ce; Figs. 8A,B, 11A–D) moderately sized, kidney shaped, rather elongate in vertical direction; with nearly round, distinctly convex, cuticular lenses; longitudinal central region more prominent than marginal areas. Frons (fr; Fig. 8A) short, triangular, enclosed by distinct, short and straight frontal sutures (fs; Fig. 8A); frontal sutures meet posterolateral clypeal margin anteriorly, distinctly separated from oblique anterolateral antennal articulatory areas; frontal tubercles absent. Coronal suture present, fairly distinct on anterior half of head capsule, obliterated posteriorly (cs; Fig. 8A). Vertex (vx; Fig. 8A) not separated from genal region; rather shallow rounded prominence on posterior margin flanked by shallow paired emarginations. Genal region posterior to compound eyes largely smooth, with indistinct, irregular vertical furrows. Frontoclypeal ridge (fcr; Fig. 11E) well developed internally; externally visible as a shallow furrow. Clypeus (cl; Figs. 8A, 11E) undivided, very short, about 10 × as wide as long; lateral margin distinctly separated from anterolateral edge of head capsule; anterior edge very slightly convex. Anterior tentorial groove not visible externally. Subgenal ridge absent. Antennal insertions broadly separated, insertion area covered by oblique edge in dorsal view; anteriorly, ventrally and posteriorly enclosed by deep and very distinct furrow. Distinct bulge present between lateral mandibular articulating area and compound eye, and posterior to shallow maxillary groove; latter section separated from adjacent parts of ventrolateral head capsule by deep furrow. Gula present, transversely extended, short and broad, enclosed by very deep posterior tentorial pits; anteriorly completely fused with large submentum; internal gular ridge short, connected with base of posterior tentorial groove. Foramen occipitale large dorsally but distinctly less wide than maximum width of head capsule; dorsally and laterally enclosed by well-developed postoccipital ridge. Internal surface of frons with a Y-shaped sclerotized structure with short basal part.

Cephalic endoskeleton. Nearly straight and simple tentorial bars (tb; Fig. 11E) arise from massive posterior base of tentorium, which is continuous with short gular ridge mesally and with well-developed postoccipital ridge laterally (por; Fig. 11E). Short anterior arms form nearly 90° angle with tentorial bars, attached to frontoclypeal ridge near anterior mandibular articulation. Posterodorsally oriented dorsal arms (dta; Fig. 11E) arise from anterior arms; apical part attached to posterior frons. Corpora tentorium absent.

Labrum and epipharynx. Labrum (lb; Figs. 8, 11E) sclerotized, short, approximately trapezoid, with strongly rounded anterolateral edges and median emargination; movably attached to anterior clypeal margin by internal membranous fold; strongly developed, elongate tormae

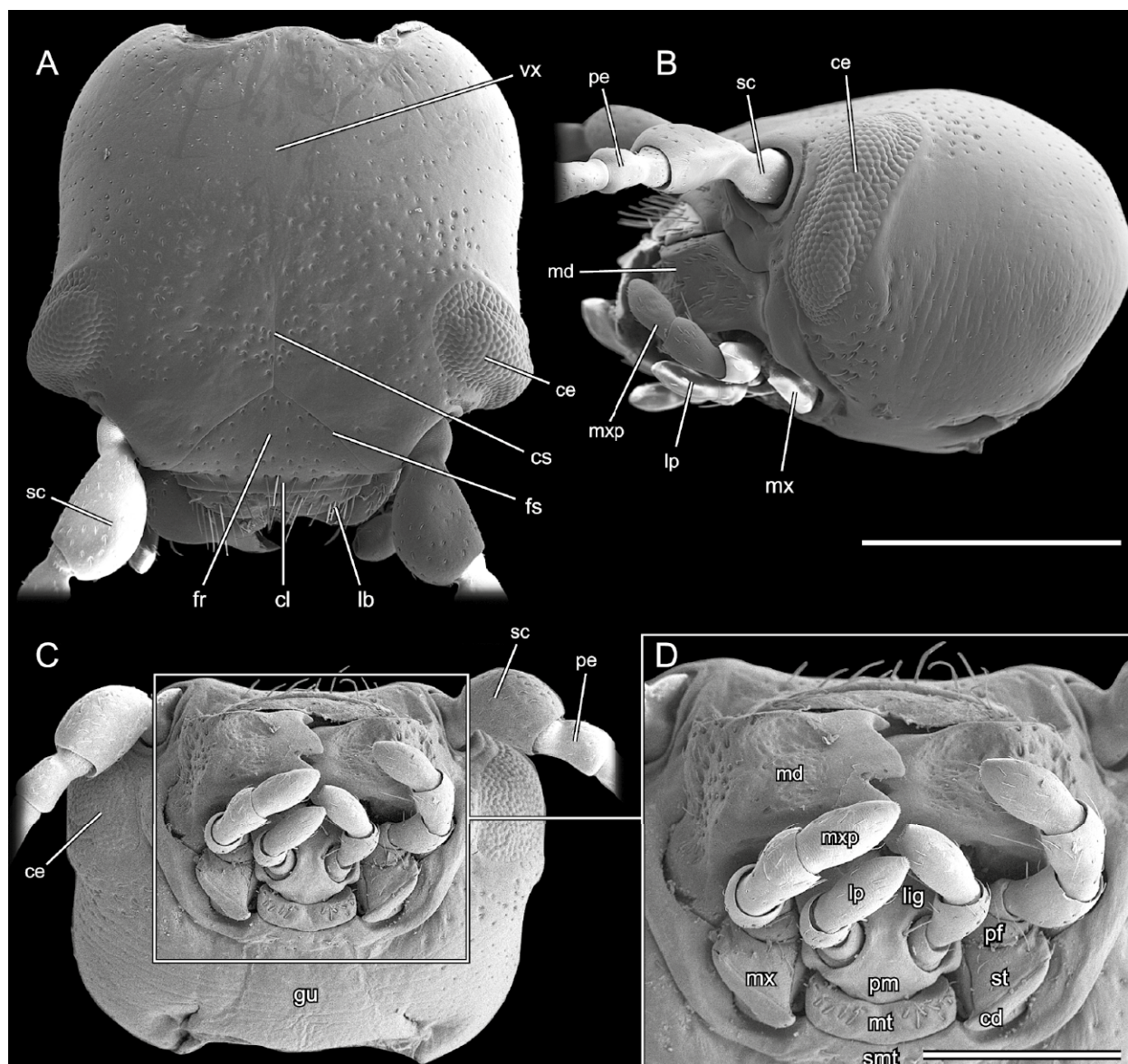


Fig. 8. Adult of *Chrysomela populi*, SEM micrographs. **A:** head, dorsal view; **B:** head, lateral view; **C:** head, frontal view; **D:** mouthparts, frontal view. — **Abbreviations:** cd: cardo; ce: compound eye; cl: clypeus; cs: coronal suture; fr: frons; fs: frontal suture; gu: gula; lb: labrum; lbr: labrum; lig: ligula; lp: labial palp; md: mandible; mt: mentum; mx: maxilla; mxp: maxillary palp; pe: pedicellus; pf: palpifer; pm: prementum; sc: scapus; smt: submentum; st: stipes; vx: vertex. Scale bar: 1 mm.

(to; Fig. 11E) protrude deeply into lumen of head capsule from posterolateral labral edges. Numerous very short sensilla inserted medially on anterior margin; upper surface with six symmetrically placed setiferous punctures. Lateral and anterolateral margin without bristles or spines. Epipharynx membranous, with well-developed median longitudinal bulge.

Antennae. Inserted below oblique anterolateral edge of head capsule (Fig. 9A), anterior to upper part of compound eyes; antennifer not present. Moderately long, posteriorly almost reaching bases of elytra, composed of scapus, pedicellus, and nine flagellomeres. Scapus (sc; Figs. 8A–C, 9A) longer than all other antennomeres except for apical one; globular and glabrous articulatory part separated from larger club-shaped distal portion by

distinct impression; anterior edge strongly rounded, posterior edge almost straight; surface of distal part smooth, with relatively scarce vestiture of punctures. Pedicellus (pe; Figs. 8B, 9A) much smaller than scapus, shorter than following antennomeres; with narrower basal part and distinctly widening, larger distal portion; vestiture similar to that of distal scapus and next three antennomeres. Flagellomere 1 similarly shaped as pedicellus but distinctly longer and less broad apically; with distinct ring-shaped basal bulge (fl1; Fig. 9A–B); flagellomere 2 similar but slightly shorter and lacking bulge (fl2; Fig. 9A); flagellomere 3 similar in shape to 2; flagellomere 4 shaped like elongate cup; with smooth basal part and widened and densely pubescent distal portion; following four flagellomeres similar, but increasing in size and

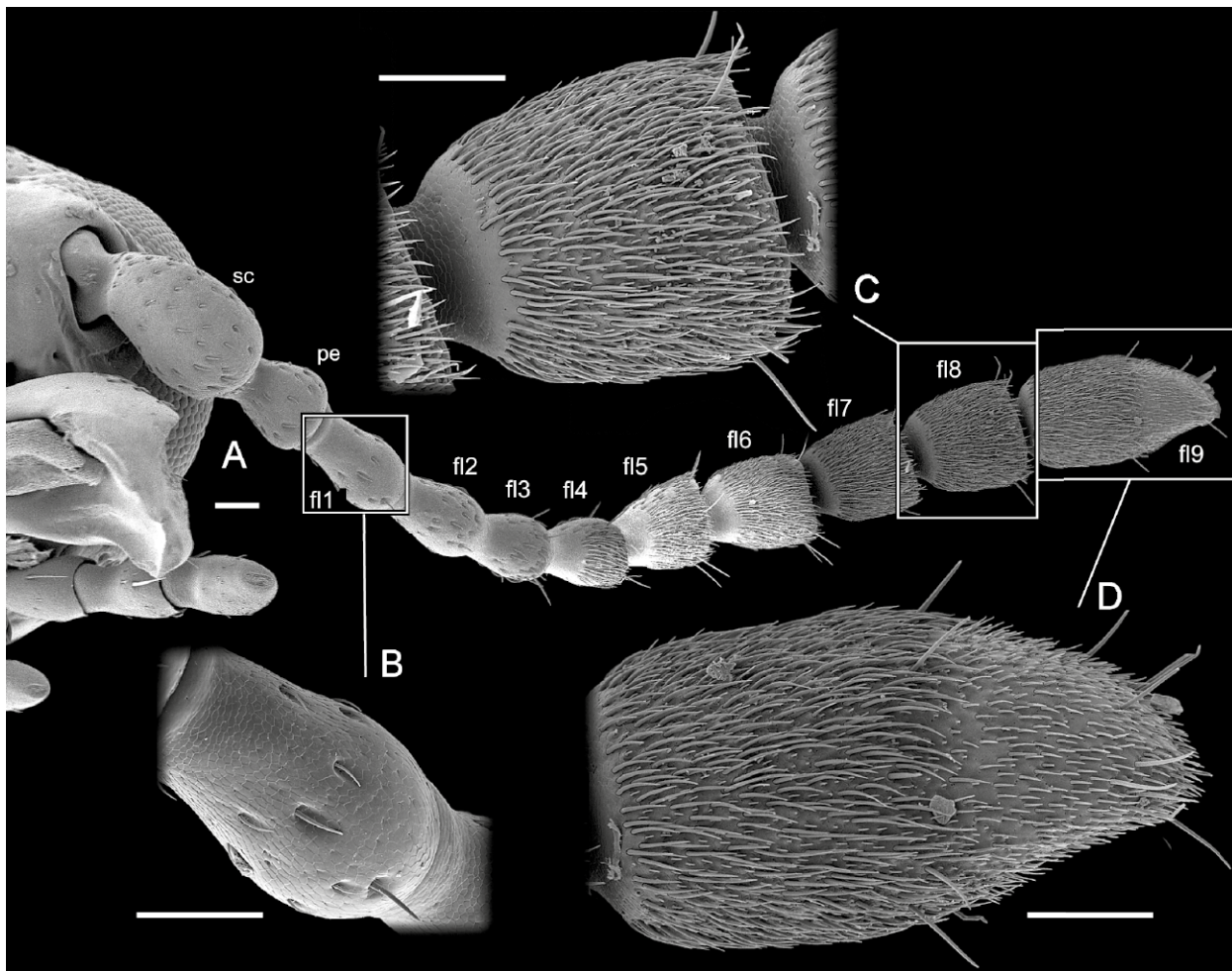


Fig. 9. Adult of *Chrysomela populi*, SEM micrographs. **A:** antenna; **B:** 1st flagellomere; **C:** 8th flagellomere; **D:** 9th flagellomere. — **Abbreviations:** fl1, 2, 3, 4, 5, 6, 7, 8, 9: flagellomeres; pe: pedicellus; sc: scapus. Scale bar: 0.5 mm.

glabrous basal portions progressively shorter (Fig. 9C); apical antennomere about as large as scapus; with short glabrous basal part; middle region cylinder-shaped (Fig. 9D).

Mandibles. Slightly asymmetric mandibles (md; Figs. 8B,D, 10A–C, 11C,F–G) with typical dicondylic articulation with strongly developed ventral condyle. Strongly sclerotized, stout, roughly triangular in dorsal view, with rounded lateral margins. External side broad at base and narrowing anteriorly, basally shallowly concave, with punctures; additional oblique and parallel-sided concavity present on middle region of external side. Distal part of mandible divided into three strongly developed, roughly triangular teeth arranged in a vertical row (Fig. 10A–C); middle tooth larger than others, with oblique, slightly irregular edge; dorsal tooth about equally long, more acuminate; ventral tooth quite distant from mandibular apex and blunt. Mesal side of mandible extensive and slightly concave, with large, concave membranous lobe densely covered with microtrichia (ml; Fig. 10B).

Maxillae. Maxilla (mx; Figs. 8D, 11B) composed of cardo (ca; Fig. 10D), subdivided stipes (ca; Fig. 10D), galea (ga; Fig. 10D), lacinia (la; Fig. 10D) and palp.

Cardo small, subtriangular, with oblique anterior edge; surface smooth, lacking spines or punctures. Stipes divided into basi- and mediostipes by basally obliterated suture. Basistipes shaped like elongate triangle; shortest side connected with anterior cardinal edge. Shape of mediostipes similar but with reversed orientation. Lacinia articulates with distinct mesal prominence of basistipes; curved; ventral surface of distal part with vestiture of extremely small, fine microtrichia. Proximal galeomere parallelogram-shaped in ventral view, completely fused with distal mediostipes; distal galeomere inserted into distal articulation area of galeomere 1; apically rounded. Palpifer laterally adjacent with distal basistipes and proximal galeomere; comparatively small but distinctly visible in ventral view and well-sclerotized. Palp (mxp; Figs. 8B,D, 10D, 11B–D,F) composed of four relatively broad segments, longer than distance from cardinal base to distal margin of galea; palpomere 1 short, inserted on palpifer; palpomere 2 about twice as long, distally widening, with strongly convex posterior margin, thus appearing curved inwards; with one long seta and several shorter ones; palpomere 3 similarly shaped but slightly shorter; palpomere 4 about as long as 2, spindle-shaped;

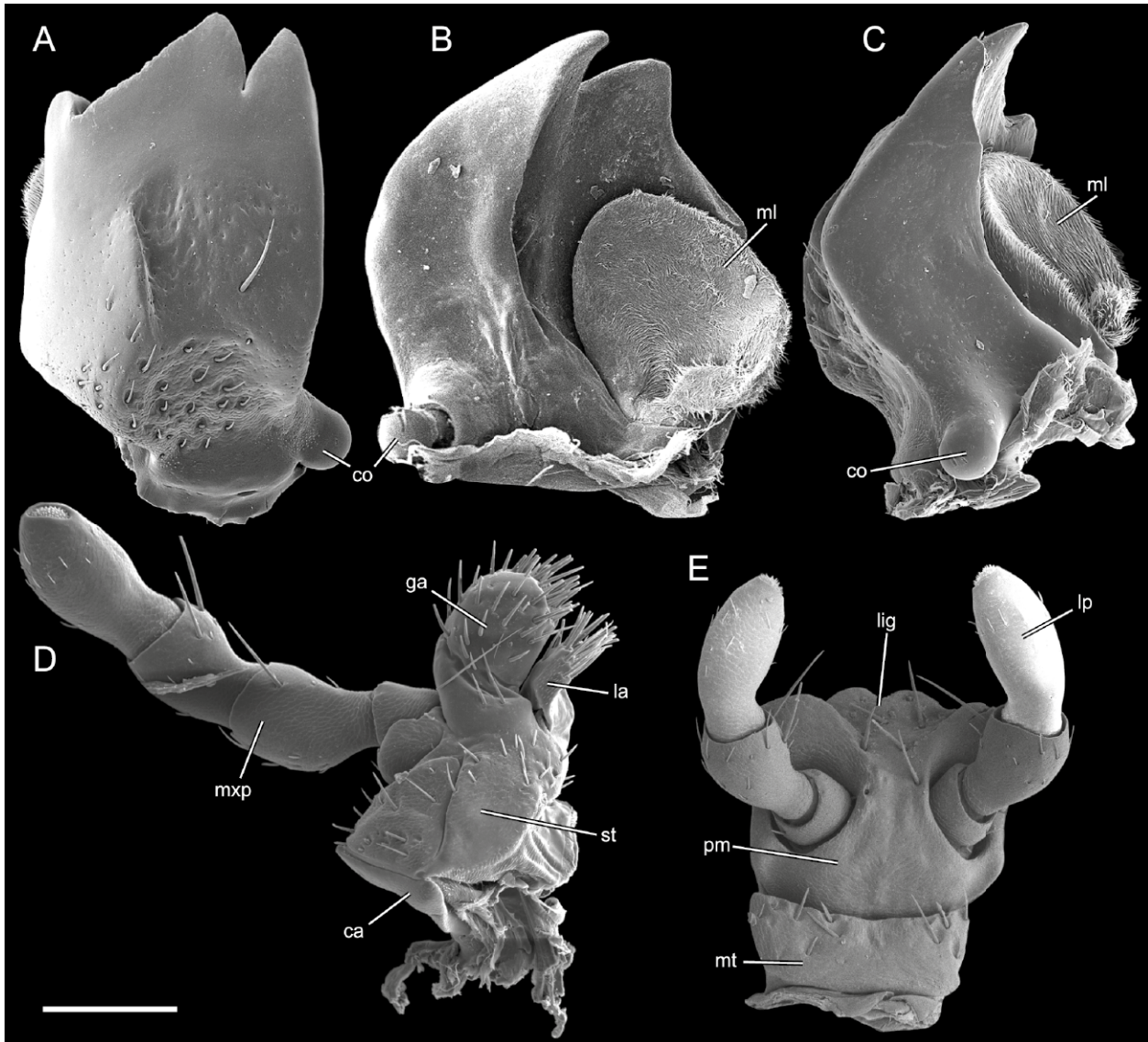


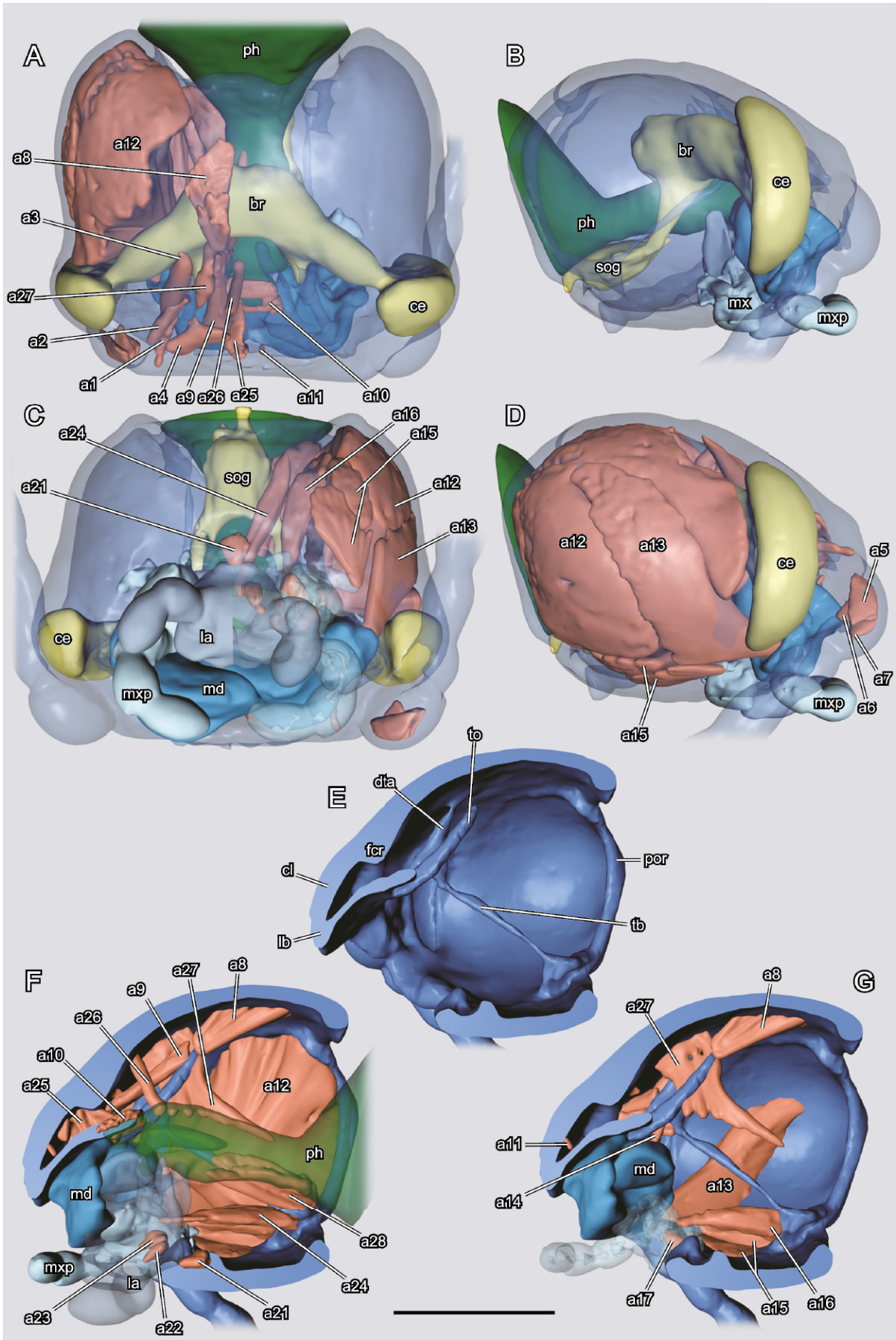
Fig. 10. Adult of *Chrysomela populi*, SEM micrographs. **A:** mandible, dorsal view; **B:** mandible, ventral view; **C:** mandible, lateral view; **D:** maxilla; **E:** labium. — **Abbreviations:** ca: cardo; co: condyle; ga: galea; la: lacinia; lig: ligula; lp: labium palp; mnt: mentum; mxp: maxilla palp; ml: membranous lobe. Scale bar: 0.2 mm

widening after shallow constriction in proximal third; evenly narrowing towards apex; surface with microreticulation; apical region rounded, with anteriorly oriented, sharply delimited oblique sensorial area with numerous minute sensilla; apex with digitiform sensilla.

Labium. Labium composed of submentum, mentum and prementum. Submentum large, fused with adjacent regions of head capsule laterally; posterior part moderately converging anteriorly, laterally delimited by rather indistinct furrow; anterior part adjacent to maxillary articulating area, lacking defined lateral border. Mentum small, transverse, inserted between stipites (mnt; Figs. 8B,D, 10D); connected with anterior submental margin by internal membrane; anterior and posterior margins almost straight. Anterior labium fused with hypopharynx, both forming a labiohypopharyngeal complex or prelabium; salivary duct appears dorsoventrally compressed in

cross section, with outer edges slightly bent downwards. Prementum well-developed, about as large as mentum; ventral surface glabrous; cranial edge bilobed (ligula), enclosed by paired extensions formed anterior to insertion areas of palps. Palpiger not present as separate, defined sclerite. Labial palp (lp; Figs. 8B,D, 10E) similar to maxillary palp, but 3-segmented and shorter; palpomere 1 short and stout, cylindrical; palpomere 2 similar to maxillary palpomere 2 but slightly smaller; apical palpomere 3 very similar to terminal maxillary palpomere, also with oblique area with numerous sensilla, short, fine setae and microreticulation.

Pharynx. Prelabium and epipharynx separate. Pharynx (ph; Fig. 11A–B,F) round in cross section, its diameter approximately 15% of diameter of head capsule. Internal surface with bulges to increase surface area. Oesophagus extremely widened in posterior region of head capsule.



← **Fig. 11.** Adult of *Chrysomela populi*, 3D reconstructions of internal structures. **A:** dorsal view, cuticle rendered transparent; **B:** lateral view, cuticle rendered transparent, muscles removed; **C:** ventral view, cuticle rendered transparent, right half of labium and right maxilla rendered transparent; **D:** lateral view, cuticle rendered transparent; **E:** midsagittal section, head capsule only; **F:** midsagittal section, pharynx and labium rendered transparent; **G:** midsagittal section, pharynx, labium and parts of musculature removed, maxilla rendered transparent. — **Abbreviations:** a1–a27: musculature; br: brain; ce: compound eye; cl: clypeus; dta: dorsal tentorial arm; fcr: frontoclypeal ridge; la: labium; lb: labrum; md: mandible; mx: maxilla; mxp: maxillary palp; ph: pharynx; por: postoccipital ridge; sog: suboesophageal ganglion; tb: tentorial bar; to: torma. Scale bar: 1 mm.

Table 3. Musculature of the adult of *Chrysomela populi*.

Number	Origin	Insertion	Function
a1	along entire dorsal tentorial arm	ventrally on basal edge of scape	depressor of the antenna
a2	dorsal area of corpotentorium	dorsally on basal edge of scape	levator of the antenna
a3	dorsal tentorial arm	laterally on basal edge of scape	depressor and rotator of the antenna
a4	mesal frons, directly posterad epistomal ridge	dorso-mesally on basal edge of scape	levator and rotator of the antenna
a5	dorsal scapal wall	lateral edge of pedicel	extensor of the flagellum
a6	dorsal scapal wall, mesad a5	ventro-mesal edge of pedicel	flexor of the flagellum
a7	dorsal scapal wall, mesad a6	dorso-mesal edge of pedicel	flexor of the flagellum
a8	dorsal head capsule	distal tip of elongate tormae	depressor of the labrum
a9	epistomal ridge	distal tip of elongate tormae, near a8	levator of the labrum?
a10	anterior torma	anterior torma of opposite side, thus overspanning anterior pharynx	?
a11	labral wall	dorsal epipharyngeal wall	dilator of the epipharynx
a12	entire lateral head capsule	with a tendon on median mandibular wall	adductor of the mandible
a13	latero-ventral head capsule	with a tendon on lateral mandibular wall	abductor of the mandible
a14	distal edge of torma	postero-mesal edge of mandible	adductor of the mandible?
a15	in 2 distinct bundles on ventral head capsule, partly on the posterior tentorial arms	cardinal process, bundle 1 on edge of the process, bundle 2 on its distal margin	promotor of the maxilla
a16	base of dorsal tentorial arms	basal edge of lacinia	adductor of the lacinia
a17	mesal stipital wall	basal edge of first maxillary palpomere	flexor of the maxillary palp
a18	basal edge of palpomere 1	basal edge of palpomere 2	flexor of the 2 nd palpomere
a19	basal edge of palpomere 2	basal edge of palpomere 3	flexor of the 3 rd palpomere
a20	basal edge of palpomere 3	basal edge of palpomere 4	flexor of the 4 th palpomere
a21	anterior edge of prementum	posterior premental rim	retractor of the prementum
a22	basal prementum	mesal edge of labial palp	adductor of the labial palp
a23	basal prementum, close to a22	lateral edge of labial palp	abductor of the labial palp
a24	base of tentorial bar	between prementum and hypopharynx on the ligula	retractor of the labium and ligula
a25	frons	dorsal epipharyngeal wall	dilator of the cibarium
a26	anterior half of frons	dorsal pharyngeal wall	dilator of the pharynx
a27	mesally on frons, far behind a26 and anterad brain	along the entire dorsal side of pharynx, reaching below brain	dilator of the pharynx
a28	base of tentorial bar	ventro-lateral pharynx	dilator of the pharynx
a29		ring muscle layer around pharynx	constrictor of the pharynx
a30		longitudinal muscle layer along pharynx	contractor of the pharynx

Nervous system. Central pars intercerebralis of brain (br; Fig. 11A) small in relation to head size, with slightly protruding protocerebral hemispheres. Optic lobes fully developed, forming large proportion of cephalic part of central nervous system, with extensive laminae ganglionares adjacent to compound eyes. Deutocerebrum not recognisable as separate unit externally. Tritocerebral commissure present. Circumoesophageal connectives fairly elongate. Suboesophageal ganglion (sog; Fig. 11C) about as wide as submentum, located in posteroventral head region.

Musculature. The musculature of the adult is illustrated in Fig. 11 and described in Table 3.

4. Discussion

4.1. Methodological aspects and implications

Insect metamorphosis is a complex and fascinating process. From a morphological point of view its study and documentation is a great challenge as it is highly dynamic and covertly taking place within a pupal sheath. The traditional techniques for studying internal struc-

tures are dissections or histological sections. The former has narrow limitations in terms of size, the latter is time-consuming, and both are invasive (FRIEDRICH et al. 2014). Moreover, sections are technically demanding to produce and prone to artifacts such as compression and loss or folding of individual slices. Thus it is not surprising that several new and innovative methods have been developed and optimized in the last decade. They greatly increase the efficiency of morphological investigations and also facilitate the observation of insects during metamorphosis.

MAPELLI et al. (1997) investigated metamorphosis for the first time without relying on histological methods or dissections. They used magnetic resonance imaging (MRI) to document the development of an individual of *Bombyx mori* from a young larva to an adult moth with a focus on the silk glands. MRI uses nuclear magnetic resonance to visualize internal features (see HART et al. 2003 for a review of its application in entomology). This technique does not have a recognizable harmful effect on live specimens, but has a rather low spatial resolution and a weak contrast between different tissues (HART et al. 2003). MICHAELIS et al. (2005) followed this approach and studied the brain of the moth *Manduca sexta*. PELLING et al. (2009) combined MRI with optical beam deflection to study the heartbeat of a monarch butterfly during metamorphosis.

Micro-computed tomography (μ -CT) yields superior resolution but involves the application of potentially harmful X-rays. It has been used in insect morphology for more than a decade and is established as a standard technique today (DEANS et al. 2012; FRIEDRICH et al. 2014). However, it was not used to investigate metamorphosis until very recently when LOWE et al. (2013) studied the tracheal and digestive systems of live specimens of the butterfly *Vanessa cardui*. One of the reasons this approach was not used earlier is the presence of water in the live insect, which greatly reduces the contrast between different tissues thus making their distinction almost impossible. Thus LOWE et al. (2013) could only study the trachea and parts of the gut, tissues with a distinctly different density. To differentiate between soft tissues like muscles, nerves or glands, samples have to be dried at the critical point or dehydrated with suitable chemicals. Even though this is obviously not possible with live material, we followed this approach in the present study to document skeleto-muscular changes during metamorphosis for the first time using μ -CT. As a result, we could not follow the development of single individuals over several stages as in the studies on *Bombyx mori*, *Manduca sexta* and *Vanessa cardui* (MAPELLI et al. 1997; MICHAELIS et al. 2005; LOEW et al. 2013). Nevertheless, this approach is highly efficient for documenting internal structures of different developmental stages, allowing a detailed comparison between them. In future studies it will be a valuable tool to investigate a series of sequential pupal stages, which will eventually lead to a much more detailed description of the dynamic process of metamorphosis than was previously possible.

4.2. Developmental transformations of cephalic structures

The main focus of this study was the detailed documentation of transformations in the skeleto-muscular system between different developmental stages of the flower beetle *Chrysomela populi*. The head morphology of the larva and adult differ extensively and nearly all character systems are affected by metamorphosis. In Table 4 the muscles are homologized between the stages and Table 5 summarizes all observed differences.

The specialization of larvae and adults for life in different habitats and microhabitats and on diverse food substrates results in a reduced intraspecific competition between these stages. This was addressed as one factor contributing to the unparalleled evolutionary success of Holometabola (e.g., GRIMALDI & ENGEL 2005; BEUTEL et al. 2011). It is also conceivable that a division of labor between developmental stages may have resulted in selection for reduced equipment in larvae, which do not need elaborate sense organs such as those on the antennae of adults or the compound eyes and no organs for dispersal over long distances. In Chrysomelidae (and most other endopterygotes) the main function of the phytophagous larva is feeding and accumulation of energy-rich substances in its fat body, whereas the principal functions of the adults are dispersal and reproduction (CHEN 1964). Our study reveals how these divergent functions affect the metamorphosis of different structural elements of the head.

In the larva the digestive system is greatly enlarged, and the diameter of the pharynx is at least 52% that of the entire head capsule, compared to only 15% in the adult. Due to the tremendously enlarged larval cephalic foregut and the resulting limitation of space in the remaining parts of the head, portions of the cephalic nervous system are shifted into the prothorax. The larval mandibles are equipped with 5 distal teeth with serrate lateral edges, which allow them to cut leaf surfaces efficiently. *Chrysomela populi* feeds on Chinese white poplar (*Populus tomentosa*) in all four active stages (note: the pupa doesn't feed so only the 3 larval and the adult stage consume food) (YU et al. 1996). However the larvae prefer fresh and thus softer leaves while adults usually feed on older ones with a thicker cuticle and cell walls (pers. obs. S.-Q. Ge). The role of the membranous basal lobe of the adult mandible (Fig. 10B,C) in this context remains unclear. As an unsclerotized structure it is probably not suitable for grinding more solid substrates (YU et al. 1996).

The most conspicuous change affects the orientation of the head: the larva is orthognathous while the adult is subprognathous. The larval legs, especially the prothoracic ones are very short (Fig. 1A). Thus the body is almost adjacent to the surface of the leaf and the larva feeds directly on the portion below its ventrally directed mouthparts (pers. obs. S.-Q. Ge). There is no easy functional explanation for the subprognathous head of adults. The body with its distinctly longer legs is held well above

Table 4. Homologisation of the musculature of *Chrysomela populi* with the terminology of WIPFLER et al. (2011).

Number	Name	Larva	Pupa	Adult
0an1	<i>M. tentorioscapalis anterior</i>	l1	p1	a1
0an2	<i>M. tentorioscapalis posterior</i>		p2	a2
0an3	<i>M. tentorioscapalis lateralis</i>		—	a3
0an4	<i>M. tentorioscapalis medialis</i>		—	a4
0an6	<i>M. scapopedicellaris lateralis</i>	—	p3	a5
0an7	<i>M. scapopedicellaris medialis</i>	—	p4	a6 + a7
0lb2	<i>M. frontoepipharyngalis</i>	l2	p5	a8 + a9?
0lb4	<i>M. labralis transversalis</i>	—	—	a10
0lb5	<i>M. labroepipharyngealis</i>	—	—	a11
0md1	<i>M. craniomandibularis internus</i>	l3	p6	a12
0md3	<i>M. craniomandibularis externus posterior</i>	l4	p7	a13?
0md6	<i>M. tentoriomandibularis lateralis inferior</i>	—	—	a14?
0mx1	<i>M. craniocardinalis</i>	—	p8	a15
0mx2	<i>M. craniolacinalis</i>	l8	p9	a16
0mx3	<i>M. tentoriocardinalis</i>	l5	—	—
0mx4	<i>M. tentoriostipitalis anterior</i>	l7?	—	—
0mx5	<i>M. tentoriostipitalis posterior</i>	l6	—	—
0mx6	<i>M. stipitolacinalis</i>	l9	—	—
0mx8–10	<i>M. stipitopalpalis</i>	l10	p10	a17
0mx12	<i>M. palpopalpalis maxillae primus</i>	—	—	a18
0mx13	<i>M. palpopalpalis maxillae secundus</i>	—	—	a19
0mx14	<i>M. palpopalpalis maxillae tertius</i>	—	—	a20
0la5	<i>M. tentoriopraementalis</i>	l11	p12	—
0la8	<i>M. submentopraementalis</i>	—	p11	a21
0la13	<i>M. praementopalpalis internus</i>	—	—	a22
0la14	<i>M. praementopalpalis externus</i>	—	—	a23
0hy1	<i>M. frontooralis</i>	l12	—	—
0hy2	<i>M. tentoriooralis</i>	l13	p13	a24
0ci1	<i>M. clypeopalatalis</i>	l14	p14	a25
0bu2	<i>M. frontobuccalis anterior</i>	l15	p15	a26
0bu3	<i>M. frontobuccalis posterior</i>	l16	p15	a27
0bu5	<i>M. tentoriobuccalis anterior</i>	l17	—	—
0bu6	<i>M. tentoriobuccalis posterior</i>	l18	—	—
0ph2	<i>M. tentoriopharyngealis</i>	l19	p16	a28
0st1	<i>M. annularis stomodaei</i>	l20	—	a29
0st2	<i>M. longitudinalis stomodaei</i>	l21	—	a30

the plant surface (Fig. 1C). Thus the beetles have to bend their heads downward to feed on the leaf they stand on (pers. obs. S.-Q. Ge) although other chrysomelid adults usually feed on the leaf margins. It is likely that the subprognathous orientation is simply a relatively slight modification of the prognathous condition, which is a groundplan feature of adult Coleoptera.

The change in head orientation has profound consequences for the cephalic morphology: with the lifting of the mouthparts resulting in an almost horizontal orientation of the head capsule, a posteroventral gap between the posterior margin of the ventral mouthparts and the foramen occipitale has to be closed by an additional structure. This is the gula of adults, which not only closes the head ventrally but also increases mechanical stability in the ventral head area between the right and left hemispheres. Thus it functionally replaces the corpotentorium, which provides this support in the larva, but which is reduced in adults, along with the muscles originating

on it (*M. tentoriobuccalis anterior* and *posterior*, *M. tentoriocardinalis*, *M. tentoriostipitalis anterior* and *posterior*, *M. tentoriopraementalis*). These muscles are partly replaced by others: *M. submentopraementalis* of adults functions as a premental retractor instead of the larval *M. tentoriopraementalis*. *M. craniocardinalis* of adults is present instead of the larval *M. tentoriocardinalis*, but in this case both muscles have a different function. The distinct subdivision of the postmentum into a well-defined mentum and submentum in adults is possibly also related to the modified orientation of the mouthparts.

Flight capacity and the necessity to find a potential mating partner requires a far more complicated sensory system in the adult than is present in larvae: instead of simple stemmata, complex compound eyes are present. This change in the visual system also requires strong modifications in the brain, notably in the optic lobes which greatly increase in size. The antennae are greatly elongated in adults and the number of antennomeres is increased from three to eleven. To ensure controlled movements of adult antennae a more complex muscle system is required. Four extrinsic and two intrinsic muscles are present in antennae of adults, whereas only one extrinsic bundle is present in those of larvae. It is conceivable that the absence of the anterior and dorsal tentorial arms in larvae is related to the greatly reduced condition of the extrinsic antennal muscles as the only larval muscle originates on head capsule cuticle. The labial and maxillary palps bear one additional segment each and their movability is increased. Intrinsic muscles are present in the adult maxillary palp and the labial palp is controlled by two extrinsic muscles absent in larvae.

In addition to modifications more or less closely related to the different functional requirements of the developmental stages, the adults exhibit some differences which cannot be easily explained in such context. The adult labrum is characterized by strongly elongate tormae and a more complex musculature obviously resulting in increased movability. The comparatively restricted movability of the labrum of larvae is seemingly in conflict with their function as the main feeding stages. This possibly relates to the reduced complexity of most larval cephalic and postcephalic body parts, which is likely a derived groundplan features of Holometabola (e.g., BEUTEL et al. 2011). Holometabolan larvae display a minimum of structural complexity, which allows them to fulfill their necessary function of feeding, but reduces investment in developing complicated structures only useful in adults. Such also applies to characters of the maxillary and labial palps and the posterior labium.

The mouthparts differ in several aspects between larvae and adults. Most changes are likely associated with the different tasks of these life stages and have been discussed above. The undivided larval mala is replaced with separate endite lobes in the adults, the laciniae and galeae. These larval features apparently have a historical background and the functional significance of the fusion is difficult to assess. In the larval groundplan of Coleoptera and Polyphaga the lacinia and galea are clearly

separate (BEUTEL 1997), whereas an undivided mala is almost universally present in larvae of the extremely diverse Cucujiformia (e.g., LESCHEN et al. 2010; LESCHEN & BEUTEL 2014), to which the Chrysomeloidea belong. This is probably an apomorphy of a very large subunit of Cucujiformia and this derived condition is preserved in Chrysomelidae (CROWSON & CROWSON 1996). In addition to muscular changes associated with reduction of the corpotentorium (see above), *M. stipitolacinalis* is present in larvae but not in the adults. This is surprising as one would assume that separate endite lobes in the adult would require more muscular control than in the larva with its undivided mala.

Morphological changes occurring in beetles during metamorphosis are insufficiently known: the larva and adult of the ptiliid *Mikado* sp. were compared by POLILOV & BEUTEL (2009) and those of the corylophid *Sericoderus lateralis* by POLILOV & BEUTEL (2010). These species differ in several ways from *Chrysomela populi*: both the larvae and adults are prognathous, and consequently several changes associated with the reorientation of the head capsule in *Chrysomela* do not occur: the gula is absent in adults of *Mikado*, whereas it is present and fused with the head capsule in adults and larvae of *Sericoderus*. The tentorial bridge is present in all stages of both species. Larval anterior tentorial arms are present in *Mikado* while they are absent in *Sericoderus* and *Chrysomela*. The larval antennal muscles of *Mikado* originate on the anterior tentorial arm in contrast to *Chrysomela*, and only the dorsal tentorial arm is missing (no information provided for *Sericoderus*; POLILOV & BEUTEL 2009). This confirms that the presence of anterior tentorial arms in larvae is related to their function as area of origin of antennal muscles.

Other features are similar in all three species: in adults the number of antennomeres increases to 11 (versus three in the larvae), a 4th maxillary palpomere is present, the volume of the digestive system strongly decreases, and the volume of the elements of the central nervous system increases.

The functional forces driving morphological change between larvae and adults of *Chrysomela* – mainly feeding in the larval stages and dispersal and mating in adults, associated with greatly improved sensory (and locomotor) organs – is similar in *Mikado* and *Sericoderus*. However, miniaturization and the resulting limitation of space also play an essential role in these two very small species, especially in the minute first instar larvae (POLILOV & BEUTEL 2009, 2010).

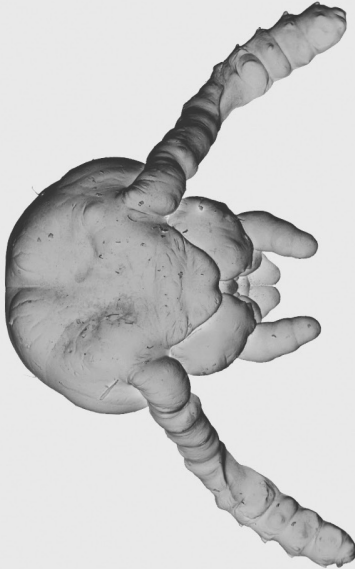
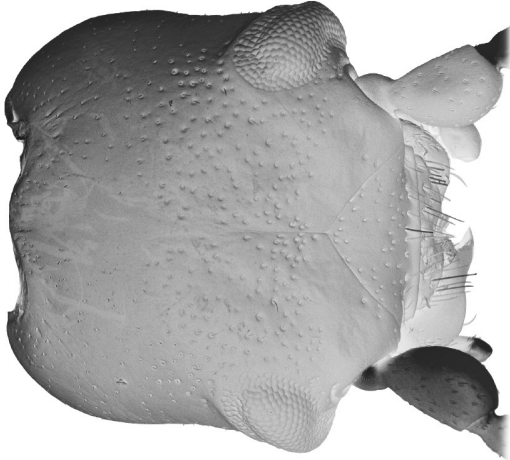
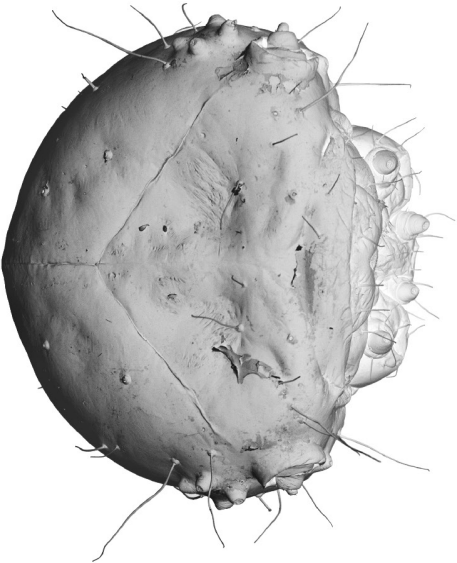
4.3. The pupa

Within the 4th day pupal sheath the pharate adult shows an interesting combination of larval and adult characters. Table 5 provides an overview of similarities and differences between these stages. In general the pharate adult resembles the adult in almost all skeletal elements including sclerotized elements of the compound eyes, the

11-segmented antennae, the mandible, the maxilla with separate endite lobes and a 4-segmented palp, the presence of a gula, the distinctly subdivided postmentum, and the presence of anterior and dorsal tentorial arms. The only difference found in a skeletal element is the shorter tormae. Aside from these skeletal features, a major transformation takes place in the orientation of the head. The larva is clearly orthognathous with an angle of approximately 87° between the longitudinal body axis and the longitudinal axis of the mouthparts. The adult is subprognathous with an angle of 154°. After 4 days of pupation the head and mouthparts of the pharate adult form an angle of 128° with the longitudinal body axis, a position intermediate between the other two. We therefore assume that the anterior orientation of the mouthparts is a continuous shift rather than a sudden reorientation, and takes place more or less continuously during the six days of pupal metamorphosis. The gula of the pharate adult is not as broad as in the adult. This is possibly related to the incomplete anterior shift of the mouthparts. To confirm these hypotheses, a more detailed study of a sequence of pupal stages would be required.

The advanced skeletal modifications of the pupa stand in sharp contrast to the condition of most internal soft parts. The very large larval foregut is already strongly reduced in size: the pharynx occupies at least 50 % of the diameter of the larval head capsule but only 19% in the pupa (day 4) and 15% in the adult. In contrast to this, the musculature and nervous system lag behind in their development. Even though ommatidia of the compound eyes are already present in the pharate adult, the optic lobes are still largely undeveloped and individual nerve cords can still be distinguished, in contrast to the adult where they are fused into a single compact structure. The musculature of the pharate adult appears also intermediate between those of the last instar larva and the adult. Most pupal muscles are much smaller than the corresponding larval or adult ones (e.g., *M. craniomandibularis internus* and *externus*) and they appear frayed or do not attach to the head capsule cuticle. In general, five categories of muscle transformations during metamorphosis can be distinguished (HEMING 2003: fig. 10.10). In addition to muscles which only exist either in the larva or adult, three types are present in both life stages: those which pass unchanged in function and form from larva to adult, those which are respecified in function and those which disintegrate completely and are replaced by a newly formed muscles (HEMING 2003: 10.2.2.1). As we studied only a single, 4 day pharate adult we were unable to follow the individual fate of each muscle and to distinguish between these types. The only exceptions are *M. annularis stomadei* and *M. longitudinalis stomodei*. As they are absent in the studied pharate adult but present in both larva and adult they apparently belong to the last type. This is consistent with a sequence described for the honey bee, where these foregut muscles begin to disintegrate after 45 hours and are replaced by adult muscles after 70 hours (OERTEL 1930). In contrast to this, “certain unidentified muscles in the head” partly disappear and reform according to OERTEL (1930).

Table 5. Observed morphological differences and similarities between the studied life stages of *Chrysomela populi*.

last instar larva	pharate adult of 4th day pupa	adult
<p>Orthognathous: Antenna: 3-segmented, 1 antennal muscle; Eyes: 6 stemmata; Endoskeleton: posterior tentorial arms and corpotentorium; Ventral head closure: postmentum, posteriorly adjacent with cervical membrane and foramen occipitale; Mandible: symmetrical, palmate and equipped with five teeth, without semimembranous lobe; Maxilla: mala, 3-segmented palpus; Labium: prementum & postmentum, 2-segmented palpus; Nervous system: suboesophageal ganglion partly located in thorax; Optical lobes: thin and cylindrical, branching into 6 optic nerves shortly before reaching stemmata; Pharynx: strongly elongated; Musculature: M. tentoriocardinalis, M. tentoriostipitalis posterior, M. stipitolacinalis</p>		
<p>Tormae: short; Musculature: M. tentoriopraementalis</p>	<p>In between orthognathous and subprognathous; Antenna: 4 antennal muscles; Optical lobes: individual nerve cords still distinguishable</p>	<p>Antenna: 11-segmented; Eyes: compound eyes; Endoskeleton: anterior and dorsal arms present, no posterior arms and corpotentorium; Ventral head closure: gula; Mandible: slightly asymmetric with three distinct teeth, with semimembranous lobe; Maxilla: lacinia and galea, 4-segmented palpus; Labium: prementum, mentum & submentum, 3-segmented palpus; Pharynx: normally developed; Musculature: M. scapopedicellaris lateralis, M. scapopedicellaris medialis, M. craniocardinalis, M. submentopraementalis</p>
	<p>Subprognathous; Endoskeleton: no corpotentorium; Antenna: 6 antennal muscles; Tormae: strongly elongated; Musculature: M. labralis transversalis, M. labroepipharyngealis, M. palpopalpalis maxillae primus, M. palpopalpalis maxillae secundus, M. palpopalpalis maxillae tertius, M. praementopalpalis internus, M. praementopalpalis externus</p>	

Most larval muscles originating on the corpotentorium (*M. tentoriocardinalis*, *M. tentoriostipitalis posterior*; *M. tentoriobuccalis anterior & posterior*) are already absent in the pharate adult. The only but noteworthy exception is *M. tentoriopraementalis* which originates on the gula in the pharate adult. This larval muscle is functionally replaced by *M. submentopraementalis* in the adult (see above). Interestingly, both muscles are present in the pharate adult, which confirms the hypothesis of replacement rather than a shift of origin. In the maxilla the tentorio-cardinal muscle is already replaced by *M. craniocardinalis* in the 4th day of the pupal stage. The antennal muscles show a similar intermediate condition: the intrinsic antennal muscles and two of the four extrinsic muscles are present in the pharate adult. The remaining two muscles apparently develop in later stages of metamorphosis. The same applies to the labral muscles and all palp muscles missing in the larvae: even though the additional maxillary and labial palpomeres are already present in the pharate adult, the corresponding intrinsic muscles are still lacking.

As pupal metamorphosis of *Chrysomela* lasts 6 days (YU et al. 1996), the pharate adult we studied had already completed two-thirds of this life stage. Our results show that during the first 4 days nearly all skeletal transformations in the head are completed. In contrast, the development of internal structures is clearly not as advanced. Despite the fact that the digestive system is already very similar to that of the adult, both the muscular and nervous systems show a combination of larval and adult characteristics. We thus conclude that in *Chrysomela* modifications of the skeleton and digestive system occur before those of the musculature and nervous system.

Even though insect metamorphosis is an intensively studied subject in morphology, neurology and developmental biology (SEHNAL 1985; NÜSCH 1987; SVÁCHA 1992; HARTENSTEIN 1993; SEHNAL et al. 1996; HEMING 2003: pp. 270–301), few detailed comparative morphological studies are available. A detailed and complete account of the metamorphosis of the head is still lacking for any endopterygote, even though OERTEL (1930) provided some data on transformations in the honeybee. In this species it takes 60 hours until the compound eyes and mouth parts take their definitive shape (OERTEL 1930), but the process of sclerotization is not finished until 240 hours. Detailed information on the metamorphosis of the cephalic muscles and nervous system were not provided. In the thorax it takes 150 hours until the vertical muscle fibers have a distinct external border, a stage when the head has long taken its final shape even though it is still not fully sclerotized. The fore- and midgut of the honeybee show no further change in general shape after 35 hours of pupation although it can take up to 240 hours until modifications at the cellular level are completed (OERTEL 1930).

These observations in the honeybee tentatively support our conclusions that modifications of the skeleton and digestive system occur before those of the muscular system. However, this interpretation is clearly preliminary and the observations in only two species can cer-

tainly not cover the diversity of events occurring throughout the Holometabola. Insect metamorphosis is arguably among the most complex processes in animal life and it is apparent that much more detailed comparative studies involving representatives of all principal endopterygote groups are required. Future studies involving a sequence of pupal stages and broader taxon sampling, with the methods used here, may lead to a better understanding of this remarkable phenomenon, which apparently played an important role in insect evolution (e.g., BEUTEL et al. 2011).

5. Acknowledgements

We thank Dr. Jie-Bing Zhang (Beijing Institute of Technology) and Mr. Jia-Lin Liu (Shanghai Jiaotong University, Shanghai) for help during μ -CT scanning. GSQ is supported by a grant from the National Science Fund for Fostering Talents in Basic Research (Special Subjects in Animal Taxonomy, NSFC-J1210002). BW is supported by the Chinese Academy of Sciences Fellowship for Young International Scientist (grant number 2011Y2SB05) and the National Science Foundation for Young International Scientist (grant number 31350110218).

6. References

- ARCHANGELSKY M. 1997. Studies on the biology, ecology and systematics of the immature stages of the New World Hydrophiloidea (Coleoptera: Staphyliniformia). – *Ohio Biology Survey Bulletin New Series* **12**: 1–207.
- ARCHANGELSKY M. 1998. Phylogeny of Hydrophiloidea (Coleoptera: Staphyliniformia) using characters from adult and preimaginal stages. – *Systematic Entomology* **23**: 9–24.
- BAUER A. 1910. Die Muskulatur von *Dytiscus marginalis* L. Ein Beitrag zur Morphologie des Insektenkörpers. – *Zeitschrift für wissenschaftliche Zoologie* **95**: 594–646.
- BECERRA J.X. 1997. Insects on plants: Macroevolution chemical trends in host use. – *Science* **276**: 253–256.
- BEUTEL R.G. 1997. Über Phylogenese und Evolution der Coleoptera (Insecta), insbesondere der Adephaga. – *Verhandlungen des Naturwissenschaftlichen Vereins in Hamburg NF* **31**: 1–164.
- BEUTEL R.G., FRIEDRICH F., GE S.Q., YANG X.K. 2014. *Insect Morphology and Phylogeny*. – De Gruyter, Berlin.
- BEUTEL R.G., FRIEDRICH F., HÖRNSCHEMEYER T., POHL H., HÜNEFELD F., BECKMANN F., MEIER R., MISOF B., WHITING M.F., VILHELMSEN L. 2011. Morphological and molecular evidence converge upon a robust phylogeny of the megadiverse Holometabola. – *Cladistics* **27**: 341–355.
- BEUTEL R.G., POHL H. 2006. Endopterygote systematics – where do we stand and what is the goal (Hexapoda, Arthropoda)? – *Systematic Entomology* **31**: 202–219.
- BREIDBACH O. 1987. The fate of persisting thoracic neurons during metamorphosis of the meal beetle *Tenebrio molitor* (Insecta:

- Coleoptera). – Roux's Archives of Developmental Biology **196** (2): 93–100.
- BREIDBACH O. 1988. Die Verpuppung des Gehirns – Modell Käferhirm. – Kölner Universitätsverlag, Köln.
- CHEN S.C. 1964. Evolution and classification of the chrysomelid beetles. – Acta Entomologica Sinica **13**: 469–483.
- COX M.L. 1981. Notes on the biology of *Orsodacne* Latreille with a subfamily key to the larvae of the British Chrysomelidae (Coleoptera). – Entomologist's Gazette **32**: 123–135.
- COX M.L. 1988. Egg bursters in the Chrysomelidae, with a review of their occurrence in the Chrysomeloidea and Curculionoidea (Coleoptera). – Systematic Entomology **13**: 393–432.
- COX M.L. 1996. The unusual larva and adult of the Oriental *Phaedon fulvescens* Weise (Coleoptera: Chrysomelidae: Chrysomelinae): A potential biocontrol agent of *Rubus* in the Mascarenes. – Journal of Natural History **30**: 135–151.
- CROSSLEY A.C. 1965. Transformations in the abdominal muscles of the blue blow-fly, *Calliphora erythrocephala* (Meig), during metamorphosis. – Journal of Embryology and Experimental Morphology **14**: 89–110.
- CROWSON R.A., CROWSON E.A. 1996. The phylogenetic relations of Galerucinae-Alticinae. Pp. 97–118 in: JOLIVET P.H.A., COX M.L. (eds), Chrysomelidae Biology. Volume 1: The Classification, Phylogeny and Genetics. – SPB Academic Publishing Amsterdam, New York.
- DEANS A.R., MIKO I., WIPFLER B., FRIEDRICH F. 2012. Evolutionary phenomics and the emerging enlightenment of arthropod systematics. – Invertebrate Systematics **26**: 323–330.
- EHRlich P.R., RAVEN P.H. 1964. Butterflies and plants – a study in coevolution. – Evolution **18**: 586–608.
- FARRELL B.D. 1998. “Inordinate fondness” explained: why are there so many beetles? – Science **281**: 555–559.
- FRIEDRICH F., MATSUMURA Y., POHL H., BAI M., HÖRNSCHEMEYER T., BEUTEL R.G. 2014. Insect morphology in the age of phylogenomics: innovative techniques and its future role in systematics. – Entomological Science **17**: 1–24.
- GRIMALDI D.A., ENGEL M.S. 2005. Evolution of the Insects. – Cambridge University Press, Cambridge, UK.
- HART A.G., BOWTELL R.W., KOCKENBERGER W., WENSELEERS T., RATNIEKS F.L.W. 2003. Magnetic resonance imaging in entomology: a critical review. – Journal of Insect Science (Tucson) **3**: 1–9.
- HARTENSTEIN V. 1993. Atlas of *Drosophila* development. Pp. 1–53 in: BATE M., ARIAS A.M. (eds), The Development of *Drosophila melanogaster*, Volume 2. – Cold Spring Harbor Press, New York.
- HEIDENREICH U., SCHMITZ A., SCHMITT M. 2009. Extraocular photoreceptors and frontal grooves in Criocerinae (Coleoptera: Chrysomelidae). Pp. 191–199 in: JOLIVET P., SANTIAGO-BLAY J., SCHMITT M. (eds), Research on Chrysomelidae, Volume 2. – Brill, Leiden.
- HEMING B.S. 2003. Insect Development and Evolution. – Comstock Publishing Associates (division of Cornell University Press), Ithaca, London.
- HINTON H.E. 1977. Enabling mechanisms. – Proceedings of the 15th International Congress of Entomology, Washington D.C.: 71–83.
- HÜBLER N., KLASS K.-D. 2013. The morphology of the metendosternite and the anterior abdominal venter in Chrysomelinae (Insecta: Coleoptera: Chrysomelidae). – Arthropod Systematics & Phylogeny **71**: 3–41.
- JOLIVET P.H.A., VERMA K.K. 2002. The Biology of Leaf Beetles. – Andover, Intercept Ltd.
- KLASS K.-D., RENTSCH J., RULIK B., HÜBLER N. 2011. The mesothoracic intercoxal perforation in Chrysomelinae and its evolutionary significance (Insecta: Coleoptera: Chrysomelidae). – Zoologischer Anzeiger **250**: 89–101.
- KORSCHOLT E. 1923, 1924. Bearbeitung einheimischer Tiere. Erste Monographie: Der Gelbrand *Dytiscus marginalis* L. Bd. 1 (1923), Bd. 2 (1924). – W. Engelmann, Leipzig.
- KRISTENSEN N.P. 1999. Phylogeny of endopterygote insects, the most successful lineage of living organisms. – European Journal of Entomology **96**: 237–254.
- LESCHEN R.A.B., BEUTEL R.G. 2014. Handbook of Zoology, Vol. IV Arthropoda: Insecta. Part 39. Coleoptera, Vol. 3: Morphology and Systematics (Phytophaga). – Walter De Gruyter, Berlin, New York.
- LESCHEN R.A.B., BEUTEL R.G., LAWRENCE J.F. 2010. Handbook of Zoology, Vol. IV Arthropoda: Insecta. Part 39. Coleoptera, Vol. 2: Morphology and Systematics (Elateroidea, Cucujiformia excl. Phytophaga). – Walter De Gruyter, Berlin, New York.
- LOWE T., GARWOOD R.J., SIMONSEN T.J., BRADLEY R.S., WITHERS P.J. 2013. Metamorphosis revealed: time-lapse three-dimensional imaging inside a living chrysalis. – Journal of the Royal Society Interface **10**: 1–6.
- MANN J.S., CROWSON R.A. 1981. The systematic positions of *Orsodacne* Latr. and *Syneta* Lac. (Coleoptera-Chrysomelidae), in relation to characters of larvae, internal anatomy and tarsal vestiture. – Journal of Natural History **15**: 727–749.
- MANN J.S., CROWSON R.A. 1983. On the internal male reproductive-organs and their taxonomic significance in the leaf beetles (Coleoptera, Chrysomelidae). – Entomologia Generalis **9**: 75–99.
- MANN J.S., CROWSON R.A. 1984. On the digitiform sensilla of adult leaf beetles (Coleoptera: Chrysomelidae). – Entomologia Generalis **9**: 121–133.
- MANN J.S., CROWSON R.A. 1996. Internal sac structure and phylogeny of Chrysomelidae. Pp. 291–316 in: JOLIVET P.H.A., COX M.L. (eds), Chrysomelidae Biology, Volume 1: The Classification, Phylogeny and Genetics. – SPB Academic Publishing Amsterdam, New York.
- MAPELLI M., GRECO F., GUSSONI M., CONSONNI R., ZETTA L. 1997. Application of NMR microscopy to the morphological study of the silkworm, *Bombyx mori* during its metamorphosis. – Magnetic Resonance Imaging **15**: 693–700.
- MAULIK S. 1926. The Fauna of British India, Coleoptera. Chrysomelidae (Chrysomelinae and Halticinae). – Taylor & Francis, London.
- MICHAELIS T., WATABE T., NATTO O., BORETIUS S., FRAHM J., UTZ S., SCHACHTNER J. 2005. In vivo 3D MRI of insect brain: cerebral development during metamorphosis of *Manduca sexta*. – Neuroimage **24**: 596–602.
- MITTER C., FARRELL B. 1991. Macroevolutionary aspects of insect-plant relationships. – Insect-Plant Interactions **3**: 35–78.
- NÜSCH H. 1987. Metamorphose bei Insekten: direkte und indirekte Entwicklung bei Apterygoten und Exopterygoten. – Zoologische Jahrbücher; Abteilung für Anatomie und Ontogenie der Tiere **115**: 453–487.

- OERTEL E. 1930. Metamorphosis in the honeybee. – *Journal of Morphology* **50**: 295–339.
- PELLING A.E., WILKINSON P.R., STRINGER R., GIMZEWSKI J.K. 2009. Dynamic mechanical oscillations during metamorphosis of the monarch butterfly. – *Journal of the Royal Society Interface* **6**: 29–37.
- POLILOV A.A., BEUTEL R.G. 2009. Miniaturisation effects in larvae and adults of *Mikado* sp. (Coleoptera: Ptiliidae), one of the smallest free-living insects. – *Arthropod Structure & Development* **38**: 247–270.
- POLILOV A.A., BEUTEL R.G. 2010. Developmental stages of the hooded beetle *Sericoderus lateral*is (Coleoptera: Corylophidae) with comments on the phylogenetic position and effects of miniaturization. – *Arthropod Structure & Development* **39**: 52–69.
- REID C.A.M. 1995. A cladistic analysis of subfamilial relationships in the Chrysomelidae sensu lato (Chrysomeloidea). Pp. 559–631 in: PAKALUK J., SLIPINSKI S.A. (eds), *Biology, Phylogeny, and Classification of Coleoptera: Papers Celebrating the 80th Birthday of Roy A. Crowson*. Volume 2. – Muzeum i Instytut Zoologii PAN, Warszawa.
- REID C.A.M. 2000. Spilopyrinae Chapuis: a new subfamily in the Chrysomelidae and its systematic placement (Coleoptera). – *Invertebrate Taxonomy* **14**: 837–862.
- RIVNAY E. 1928. External morphology of the Colorado potato beetle (*Leptinotarsa decemlineata* Say). – *Journal of the New York Entomological Society* **36**: 125–142.
- ROBERTSON C.W. 1936. The metamorphosis of *Drosophila melanogaster*, including an accurately timed account of the principal morphological changes. – *Journal of Morphology* **59**: 351–399.
- SAMUELSON G.A. 1996. Binding sites: Elytron-to-body meshing structures of possible significance in the higher classification of Chrysomeloidea. Pp. 267–290 in: JOLIVET P.H.A., COX M.L. (eds), *Chrysomelidae Biology, Volume 1: the classification, phylogeny and genetics*. – SPB Academic Publishing Amsterdam, New York.
- SCHMITT M. 1998. Internal head capsule morphology of Chrysomelidae (Insecta: Coleoptera). Pp. 137–153 in: BIONDI M., DACCORDI M., FURTH D.G. (eds), *Proceedings of the Fourth International Symposium on the Chrysomelidae*. – Museo Regionale di Scienze Naturali, Torino.
- SEHNAL F. 1985. Morphology of insect development. – *Annual Review of Entomology* **30**: 89–109.
- SEHNAL F., SVÁCHA P., ZRZAVY J. 1996. Evolution of insect metamorphosis. Pp. 3–58 in: GILBERT L.I., TATA J.R., ATKINSON B.G. (eds), *Metamorphosis. Postembryonic reprogramming of gene expression in amphibian and insect cells*. – Academic Press, New York.
- SUZUKI K. 1996. Higher classification of the family Chrysomelidae (Coleoptera). Pp. 3–54 in: JOLIVET P.H.A., COX M.L. (eds), *Chrysomelidae Biology, Volume 1: the classification, phylogeny and genetics*. – SPB Academic Publishing Amsterdam, New York.
- SVÁCHA P. 1992. What are and what are not imaginal discs: re-evaluation of some basic concepts (Insecta, Holometabola). – *Developmental Biology* **154**: 101–117.
- WHITE K.P. 1999. Microarray analysis of *Drosophila* development during metamorphosis. – *Science* **286**: 2179–2184.
- WIPFLER B., MACHIDA R., MUELLER B., BEUTEL R.G. 2011. On the head morphology of Grylloblattodea (Insecta) and the systematic position of the order, with a new nomenclature for the head muscles of Dicondylia. – *Systematic Entomology* **36**: 241–266.
- XUE H.J., MAGALHÃS S., LI W.Z., YANG X.K. 2009. Reproductive barriers between two sympatric beetle species specialized on different host plants. – *Journal of Evolutionary Biology* **22**: 2258–2266.
- XUE H.J., YANG X.K. 2008. Common volatiles are major attractants for neonate larvae of the specialist flea beetle *Altica koreana* (Coleoptera: Chrysomelidae). – *Naturwissenschaften* **95**: 639–645.
- YU P.Y., WANG S.Y., YANG X.K. 1996. *Economic Insect Fauna of China: 54, Coleoptera: Chrysomeloidea (II)*. – Science Press, Beijing.